Branched-Chain Amino Acid Metabolism is Regulated by ERRα in Primary Human Myotubes and is Further Impaired by Glucose Loading in Type 2 Diabetes

Rasmus J.O. Sjögren[1,a] David Rizo-Roca[1,a], Alexander V. Chibalin[1], Elin Chorell[2], Regula Furrer[3], Shintaro Katayama[4], Jun Harada[5], Håkan K.R. Karlsson[1], Christoph Handschin[3], Thomas Moritz[6], Anna Krook[7], Erik Näslund[8], and Juleen R. Zierath[1,7]

[1]Department of Molecular Medicine and Surgery, Integrative Physiology, Karolinska Institutet, Stockholm, 171 77, Sweden.

[2]Department of Public Health and Clinical Medicine, Umeå University, Umeå, 901 87, Sweden.

[3]Biozentrum, University of Basel, Basel, 4056, Switzerland.

[4]Department of Biosciences and Nutrition, Karolinska Institutet, Huddinge, 141 83, Sweden.

[5]Cardiovascular-Metabolics Research Laboratories, Daiichi Sankyo Co., Ltd., Tokyo, Japan.

[6]Swedish Metabolomics Centre, Department of Forest Genetics and Plant Physiology, Swedish University of Agricultural Sciences, Umeå 750 07, Sweden.

[7]Department of Physiology and Pharmacology, Integrative Physiology, Karolinska Institutet, Stockholm, 171 77, Sweden.

[8]Division of Surgery, Department of Clinical Sciences, Danderyd Hospital, Karolinska Institutet, Stockholm, 182 88, Sweden.

[a]These authors contributed equally.

Corresponding Author:

Juleen R. Zierath
Department of Physiology and Pharmacology &
Department of Molecular Medicine and Surgery,
Section of Integrative Physiology,
Karolinska Institutet,
Biomedicum C4
Solnavägen 9,
SE 171 77 Stockholm, Sweden
Phone: +46 (0) 8 524 875 80
Fax: +46 (0) 8 33 54 36
E-mail: juleen.zierath@ki.se

Word count: 3991

Abstract

Aims/hypothesis

Increased levels of branched-chain amino acids (BCAAs) are associated with type 2 diabetes pathogenesis. However, most metabolomic studies are limited to an analysis of plasma metabolites under fasting conditions, rather than the dynamic shift in response to a metabolic challenge. Moreover, metabolomic profiles of peripheral tissues involved in glucose homeostasis are scarce and the transcriptomic regulation of genes involved in BCAA catabolism is partially unknown. This study aimed to identify differences in circulating and skeletal muscle BCAA levels in response to an OGTT in individuals with normal glucose tolerance (NGT) or type 2 diabetes. Additionally, transcription factors involved in the regulation of the BCAA gene set were identified.

Methods

Plasma and *vastus lateralis* muscle biopsies were obtained from individuals with NGT or type 2 diabetes before and after an OGTT. Plasma and *quadriceps* muscles were harvested from skeletal muscle-specific PGC-1α knockout and transgenic mice. BCAA-related metabolites and genes were assessed by LC-MS/MS and RT-PCR, respectively. Small interfering RNA and adenovirus-mediated overexpression techniques were used in primary human skeletal muscle cells to study the role of *PGC-1A* and *ESRRA* in the expression of the BCAA gene set. Radiolabeled leucine was used to analyze the impact of ERRα knockdown on leucine oxidation.

Results

Impairments in BCAA catabolism in people with type 2 diabetes under fasting conditions were exacerbated after a glucose load. Branched-chain keto acids were reduced 37–56% after an OGTT in the NGT group, whereas no changes were detected in individuals with T2D. These

changes were concomitant with a stronger correlation with glucose homeostasis biomarkers and downregulated expression of BCAT2, BCKDH complex subunits and 69% of downstream BCAA-related genes in skeletal muscle. In primary human myotubes overexpressing PGC-1α, 61% of the analyzed BCAA genes were upregulated, while 67% were downregulated in the *quadriceps* of skeletal muscle-specific PGC-1α knockout mice. *ESRRA* (encoding estrogen-related receptor α, ERRα) silencing completely abrogated the PGC-1α-induced upregulation of BCAA-related genes in primary human myotubes.

Conclusions/interpretation

Metabolic inflexibility in type 2 diabetes impacts BCAA homeostasis and attenuates the decrease of circulating and skeletal muscle BCAA-related metabolites after a glucose challenge. Transcriptional regulation of BCAA genes in primary human myotubes via a PGC-1α is ERRα-dependent.

Keywords: Branched-chain amino acid, Estrogen-related receptor alpha, Oral glucose tolerance test, Peroxisome proliferator-activated receptor gamma coactivator 1-alpha, Type 2 diabetes, Skeletal muscle.

Abbreviations

3-HIB: 3-hydroxyisobutyrate

BCAA: branched-chain amino acid

BCKA: branched-chain α-keto acid

ERRα: Estrogen-related receptor alpha

HSMC: human skeletal muscle primary cell

NGT: normal glucose tolerance

PGC1α: Peroxisome proliferator-activated receptor gamma coactivator 1-alpha

WT: Wild type

Research in context

What is already known about this subject?

- Circulating levels of BCAA are elevated in type 2 diabetes.
- PGC-1α is involved in the transcription of the BCAA gene set.

What is the key question?

- Does metabolic inflexibility associated with type 2 diabetes encompass BCAA homeostasis and PGC-1α mediated transcription of the BCAA gene set?

What are the new findings?

- BCAA homeostasis is further compromised by a glucose challenge in type 2 diabetes.
- An OGTT reveals coordinated regulation between BCAA metabolites, blood glucose, and HbA_{1c} levels.
- ERRα is essential for PGC-1α-mediated BCAA gene expression in primary human myotubes.

How might this impact on clinical practice in the foreseeable future?

- An OGTT can be used to underscore impairments in BCAA metabolism. These findings suggest that interventions targeting the PGC-1α/ ERRα axis may improve BCAA homeostasis.

Introduction

Type 2 diabetes is a metabolic disease characterized by chronic hyperglycemia and insulin resistance [1]. These metabolic derangements severely affect pathways controlling the appropriate sensing and handling of nutrients, thereby leading to a positive energy balance and metabolic inflexibility, which further compromises whole body glucose homeostasis [2]. Overnutrition and type 2 diabetes-related disturbances also affect non-glucose metabolites such as branched-chain amino acids (BCAAs; leucine, isoleucine and valine) [3], essential amino acids whose utilization and metabolism are exquisitely regulated in healthy individuals. While BCAA and related metabolites play a role in protein synthesis, they also modulate liver gluconeogenesis and lipogenesis rates, cell growth, and nutrient signaling, and can enter the tricarboxylic acid cycle to produce energy [4]. Under pathological conditions, BCAAs, especially in a context of overnutrition, disrupt insulin sensitivity and secretion [5].

Circulating levels of BCAAs are elevated in individuals with obesity, insulin resistance and/or type 2 diabetes [6]. Metabolomic profiling of blood metabolites has revealed a signature of altered BCAA catabolism in obese individuals, with a strong association with insulin resistance [7]. BCAA-related metabolites are predictive of type 2 diabetes pathogenesis [8], as well as prognostic markers for intervention outcomes [9, 10]. Mendelian randomization analysis suggested a causal link between genetic variants associated to impaired BCAA catabolism and higher risk of type 2 diabetes [11]. Therefore, there is growing evidence that high levels of BCAAs and related intermediate metabolites are not only type 2 diabetes biomarkers, but also pathophysiological factors. However, many of these studies were conducted in individuals after an overnight fast, under conditions in which protein degradation in skeletal muscle, and a concomitant release of amino acids to support gluconeogenesis [12], could mask deeper alterations in BCAA homeostasis. Moreover, they do not provide insight into the dynamic shift in metabolism that occurs in response to nutritional challenges. An

analysis of metabolomic signatures in fasted individuals with glucose tolerance or type 2 diabetes before and after a glucose challenge may provide insight into dynamic changes in BCAAs and related metabolites and the consequences of insulin resistance.

Skeletal muscle is the largest contributor to systemic BCAA oxidation [13] and therefore impairments in glucose and BCAA metabolism in myocytes have an impact on whole body metabolic homeostasis. While BCAA-related gene expression and oxidation rates are reduced in *vastus lateralis* muscle from individuals with insulin resistance [14], studies of BCAA metabolism in human skeletal muscle are scarce. BCAA catabolism occurs in the mitochondrial matrix, implicating alterations in mitochondrial proteins may influence BCAA metabolism. In transgenic mice overexpressing the mitochondrial biogenesis inducer peroxisome proliferator-activated receptor γ (PPAR γ) coactivator 1α (PGC-1α), BCAA levels are reduced in *gastrocnemius* muscle [15]. Conversely, administration of the PPARγ agonist thiazolidinedione rosiglitazone improves glycemic control and increases circulating levels of BCAAs in individuals with type 2 diabetes [16]. Nevertheless, mechanisms underlying the direct role of PGC-1α in the regulation of BCAA catabolism are unclear.

The aim of this study was to assess whether an OGTT can further reveal an impairment in BCAA metabolism in individuals with type 2 diabetes. We also aimed at identifying a PGC-1α transcriptional partner in the regulation of the BCAA gene program by using cell and mouse models with altered PGC-1α expression.

Research Design and methods

Subjects

Thirty-two men with normal glucose tolerance (NGT) and twenty-nine men with type 2 diabetes aged 44-69 years were recruited to participate in this study. All participants gave their informed consent. The study was approved by the regional ethical review board in Stockholm. The experimental procedures were conducted according to the Declaration of Helsinki. Participants underwent a clinical health screening consisting of clinical chemistry and anthropometric measurements (Table 1 and 2). Five individuals in the control group that exhibited impaired glucose tolerance and one individual diagnosed with type 2 diabetes that exhibited NGT were excluded from the study Fig. 1. Individuals with type 2 diabetes had higher blood glucose, Hb1Ac, and HOMA-IR, as well as higher BMI and waist circumference (Table 1 and 2). Individuals with type 2 diabetes included in the transcriptomic analysis were older than the normal glucose tolerant controls (Table 2). Individuals with type 2 diabetes were treated with metformin (n=23; daily dose range 500-3000 mg) and/or sulfonylurea (n=7; daily dose range 2-5 mg). Anti-diabetic medication was taken by the individuals with type 2 diabetes after the skeletal muscle biopsy collection.

Participants arrived at the clinic at 07:45 after a 12-h fast. A catheter was inserted into an arm vein and fasting blood samples were obtained. After applying local anesthesia (Lidokain hydrochloride 5 mg/mL), biopsies from the *vastus lateralis* were obtained using a conchotome (AgnTho's AB, Sweden). After ∼15 min, participants were given a solution containing 75 g of glucose and underwent an OGTT. A blood sample was obtained 30 min after glucose ingestion. After 120 minutes, a blood sample and *vastus lateralis* biopsy was obtained. All biopsies were s immediately snap-frozen in liquid nitrogen and stored at -80°C. Metabolomic analysis was

performed by Metabolon, Inc. (Durham, NC) as described [17]. See electronic supplementary material [ESM] Methods: Human plasma and skeletal muscle metabolomics for details.

Cells culture experiments

Human satellite cells were harvested from *vastus lateralis* skeletal muscle biopsies of healthy volunteers from both sexes and differentiated as described [18]. Mouse C2C12 myoblasts (ATCC CRL-1772, VA) were propagated in growth media (DMEM, 20% FBS, and 1% anti-anti). After ~12 hours, medium was changed to differentiation medium (DMEM, 2% horse serum, and 1% anti-anti) and differentiated myotubes were cultured for six days before the final experiments. For pharmacological inhibition of ERRα, human skeletal muscle cells (HSMCs) were incubated with 5 μM of XCT-790 (X4753, Sigma-Aldrich), an inverse ERRα agonist, for 32 hours. Cells were regularly tested to confirm the absence for mycoplasma contamination.

Small interfering RNAs (siRNA) targeting *PPARGC1A* or *ESRRA* mRNA predesigned by ThermoFisher Scientific (Silencer® Select, s21395 and s4830) were used to silence the expression of these genes. Scramble siRNA (4390847, ThermoFisher) was used as negative control. Transfection of C2C12 myoblasts and HSMCs was performed 3 and 6 days after induction of differentiation, respectively, in OptiMEM reduced serum media (31985062, ThermoFisher) with Lipofectamine® RNAiMAX (13778, ThermoFisher).

Adenoviral-delivery of human and mouse PGC1α (Ad-PGC1α) or GFP (Ad-GFP) was performed over-night in differentiated HSMCs and C2C12 myotubes. Experiments were performed 48 hours after inducing transduction. In cells that were both treated with siRNA and transduced, silencing was performed as described above and cells were transduced immediately after transfection.

Mouse models

Male mice were housed under controlled lighting (12 h light/12 h dark cycle) with free access to food and water. Experiments were performed in accordance with Swiss federal guidelines and were approved by the Kantonales Veterinäramt Basel-Stadt. Skeletal muscle-specific PGC-1α transgenic mice (mTG) are described elsewhere [19]. The PGC-1α muscle-specific knockout mice (mKO) were generated by breeding PGC-1α$^{loxP/loxP}$ mice [20] with transgenic mice expressing the Cre recombinase under the control of the human α-skeletal actin promoter (HSA-Cre). Chow diet (AIN-93G; 7% fat, 58.5% carbohydrates, 18% protein and 16.5% of crude fiber, ash, and moisture) was provided by Provimi Kliba AG (Kaiseraugst, Switzerland).

Fasted (4h) male mice aged 11-14 weeks were anesthetized by intraperitoneal injection of pentobarbital (150 mg/kg) and tissues were collected. Metabolomic analysis of plasma and quadriceps muscle was performed at the Swedish Metabolomics Centre (Umeå University) as described [21]. See ESM Methods: Mouse plasma and skeletal muscle metabolomics for details.

Real-time qPCR

Total RNA from human skeletal muscle biopsies, mouse skeletal muscles and cultured myotubes was extracted for mRNA analysis of BCAA genes. See ESM Methods: RNA isolation and relative mRNA expression for details. Primer sequences are shown in ESM Table 1 and ESM Table 2.

Western blot analysis

Equal amounts of protein from human skeletal muscle biopsies (10 µg) and cells (20 µg) were analyzed for BCKDHA, p^{S293}-BCKDHA, BCKDK and PPM1K. See ESM Methods: Western Blot analysis for details.

Leucine oxidation

Myotube cultures were incubated with 1 ml of Ham's F10 Medium in the presence of 0.1 mCi/ml radiolabeled leucine (L-[U-C^{14}]-Leucine; 11.1GBq/mmol, NEC279E250UC, PerkinElmer) and either 3,6-dichlorobenzo(b)thiophene-2carboxylic acid (BT2) (ENA018104907, Sigma-Aldrich, Sweden) or DMSO. Small cups were placed in cell-culture wells and plates were air-tight sealed. After a 4-hour incubation at 37°C, 150 µL 2 M HCl and 300 µL of 2 M NaOH were added into each well and small cup, respectively. After 1 hour, the liberated CO_2 was collected and subjected to scintillation counting (Tri-Carb 4910TR, PerkinElmer, MA, USA).

Statistical Analysis

Results in tables are reported as means ± SEM. Metabolites and gene expression results are reported as Tukey boxplots with median (line), 25–75% (box) and the 25th/75th percentile minus/plus 1.5 times the inter-quartile distance (whiskers). Values outside this range are plotted as individual open circles. Outlier values detected using the Grubb's test are plotted as closed circles and were not considered in the statistical analysis. HSMCs from each donor, C2C12 myotubes at different passages, and single animals, were considered as experimental units. Data normality was tested using the Shapiro-Wilk test. Homogeneity of variance was tested using the Levene's test. Data that did not meet these criteria was transformed with Tukey's Ladder before the significance testing. Data was analyzed using GraphPad Prism software (GraphPad Software Inc.). Statistical tests and data information are indicated in the figure legends.

Results

Glucose loading further attenuates BCAA catabolism in individuals with type 2 diabetes

Metabolomic profiling reveals that a glucose ingestion in fasted individuals elicits an insulin-dependent metabolic response, that is blunted with pre-diabetes [22]. To assess whether

this impaired response also affects the BCAA profile, we measured levels of leucine, isoleucine, valine, and derived metabolites in plasma and *vastus lateralis* biopsies from individuals with either NGT or type 2 diabetes before and after an OGTT. Under fasted conditions, the three BCAAs were ~10% and ~13% higher in plasma and skeletal muscle, respectively, from individuals with type 2 diabetes as compared to NGT (Fig. 2a-c), and non-significant changes were found in the corresponding branched-chain α-keto acids (BCKAs) (Fig. 2d-f). While BCAA-derived acyl-carnitines were not different between groups (Fig. 2g-k), fasting 3-hydroxisobutyrate (3-HIB) was higher in plasma (+37%) and skeletal muscle (+45%) from individuals with type 2 diabetes as compared to NGT (Fig. 2l). This valine-derived metabolite (Fig. 2m) promotes insulin resistance in skeletal muscle cells by increasing fatty acid uptake [23].

Glucose ingestion decreased circulating and intramuscular levels of BCAA and BCKA (Fig. 2a-f, ESM Fig. 1a-b), albeit to a lesser extent in individuals with type 2 diabetes. The intramuscular content of BCKA was decreased 37–56% in individuals with NGT, whereas levels remained unaltered with type 2 diabetes. These differences were not driven by the higher BMI and age in the type 2 diabetes group (ESM Table 3). BCKA are irreversibly decarboxylated by the branched-chain α-ketoacid dehydrogenase complex (BCKDH), the rate-limiting enzyme in the catabolism of BCAA. We determined total abundance and phosphorylated (inactive) BCKDH content in skeletal muscle (Fig. 2n-q) and found no differences between groups. Glucose loading decreased 3-HIB levels in skeletal muscle of individuals with NGT, but not type 2 diabetes (Fig. 2l). Collectively, these results suggest that a glucose challenge unmasks defects at several steps of BCAA catabolism in type 2 diabetes. Indeed, circulating levels of leucine, isoleucine and derived BCKAs exhibited a positive correlation ($r = 0.64 – 0.77$) with blood glucose, HbA_{1c} levels and HOMA-IR after an OGTT (Fig. 2r-w, ESM Fig. 1c-d).

Expression of genes involved in BCAA catabolism is decreased in skeletal muscle from individuals with type 2 diabetes.

Expression of genes encoding for enzymes involved in the first steps of BCAA metabolism, namely Branched Chain Amino Acid Transaminase 2 (*BCAT2*) and three subunits of the BCKDH complex were decreased in skeletal muscle of individuals with type 2 diabetes (Fig. 3a). Furthermore, 69% of the analyzed genes participating in metabolic steps downstream BCKDH showed a similar profile (Fig. 3b), indicating that BCAA gene expression is widely downregulated in skeletal muscle of individuals with type 2 diabetes. These differences were also evident after an OGTT, as mRNA levels remained relatively stable. PGC-1α is an upstream regulator of BCAA metabolism [15]. Expression of *PPARGC1A*, which encodes for PGC-1α, was decreased in skeletal muscle of individuals with type 2 diabetes, irrespective of the feeding schedule (Fig. 3c). In addition, *PPARGC1A* was positively correlated with BCAA gene expression (ESM Fig. 2a) and BCAA metabolites in individuals with NGT but not type 2 diabetes (ESM Fig. 2b-c), while the expression of several of BCAA genes was inversely associated with blood glucose and HbA_{1c} (Fig. 3d). Expression of BCAA genes did not consistently correlate with BCAA-related metabolites (Fig. 3e) but exhibited opposite patterns in individuals with NGT and type 2 diabetes (ESM Fig. 2b-c).

PGC-1α mediates BCAA gene expression in primary human skeletal muscle cells.

Primary HSMCs transfected with *PPARGC1A* siRNA had reduced expression of *PPARGC1A* (Fig. 4a), which moderately decreased the expression of genes of the family of acyl-CoA dehydrogenases (*ACAD8*, *ACADSB*, and *IVD*), and *HIBADH* (encoding the 3-hydroxyisobutyrate dehydrogenase enzyme), as compared to cells treated with a scrambled siRNA (Fig. 4b). Adenovirus-mediated *PPARGC1A* overexpression (Ad-PGC1A) in HSMCs (Fig. 4c) increased the expression of 61% of the genes relative to adenovirus-GFP cells (Fig.

4d). We found increased PPM1K (Fig. 4f) and reduced BCKDH protein content in Ad-PGC1A cells, which was associated with a higher pBCKDHA/BCKDHA ratio (Fig. 4g-i).

Mice with skeletal muscle-specific modified expression of *PPARGC1A* exhibit altered levels of BCAA gene transcripts and related metabolites.

Muscle-specific PGC-1α knockout mice (PGC-1α mKO) had normal body weight (ESM Fig. 3a) and slightly impaired glucose tolerance (ESM Fig. 3b-c) as compared to wild-type (WT) littermates. Skeletal muscle from PGC-1α mKO mice (Fig. 5a) had decreased expression of the majority (67%) of the analyzed BCAA genes relative to controls (Fig. 5b-d). Accordingly, a contrasting profile of BCAA gene expression was observed in skeletal muscle-specific PGC-1α transgenic mice (mTg) versus the PGC-1α mKO mice, with an upregulation of the BCAA genes relative to controls (Fig. 5e-h). These gene expression changes were not associated with alterations in either body weight or glucose tolerance (ESM Fig. 3d-f).

To ascertain whether PGC-1α-associated alterations in BCAA gene expression have functional implications in BCAA metabolism, we performed LC/MS metabolomics to profile BCAA-related metabolites in plasma and *quadriceps* muscle from mKO and mTG mice. Circulating BCAA levels in mKO and mTG mice were unaltered relative to respective controls (Fig. 5i-k), whereas the intramuscular content of valine was reduced in mTG mice (Fig. 5l-n). Similar non-significant changes were observed for isoleucine (p=0.09) and isovalerylcarnitine (p=0.12) (Fig. 5m and o), while mKO mice exhibited decreased levels of 3-HIB (Fig. 5q). Consistent with our results in HSMCs, C2C12 Ad-PGC1A upregulated the expression of BCAA-related genes (ESM Fig. 3g), which was associated with increased leucine oxidation (ESM Fig. 3h).

PGC-1α regulates BCAA gene transcription through ERRα.

The orphan nuclear receptor ERRα, encoded by *ESRRA*, is a canonical functional partner of PGC-1α (Fig. 6a) that regulates metabolic processes in mitochondria [24]. Thus, we investigated whether ERRα is necessary for PGC-1α-enhanced BCAA gene expression. siRNA-mediated silencing of ERRα (Fig. 6b) decreased the expression of 65% of the analyzed genes (Fig. 6c). We determined whether this BCAA gene downregulation affects leucine oxidation in skeletal muscle. HSMCs were treated with either DMSO or BT2, a BCKDK inhibitor that increases BCAA oxidative flux. *ESRRA* silencing decreased leucine oxidation rates under BCKDH-activated conditions, as measured by CO_2 production after incubation with [U–^{14}C]-leucine (Fig. 6d). We next tested whether ERRα is a PGC-1α interacting partner in the transcriptional regulation of the BCAA gene set using HSMCs treated with either scramble siRNA or *ESRRA* siRNA and transfected with Ad-GFP or Ad-PGC1A. We also tested this using Ad-PGC-1A cells treated with the inverse ERRα agonist XCT-790 (ESM Fig. 4). Since *PPARGC1A* and *ESRRA* mutually regulate their expression, we confirmed that *ESRRA* silencing did not abrogate *PPARGC1A* in cultured cells. Ad-PGC1A cells had high levels of *PPARGC1A* transcripts regardless the treatment with *ESRRA* siRNA (Fig. 6e and ESM Fig. 4a), whereas the expression of two known targets of PGC-1α/ERRα, *TFAM* and *VEGF*, was dampened by *ESRRA* siRNA despite the overexpression of *PPARGC1A*. Knockdown and inhibition of *ESRRA* completely ablated PGC-1α-mediated upregulation in all analyzed genes (Fig. 6f-h, ESM Fig. 4b-d), indicating that ERRα is essential for the transcriptomic regulation of the BCAA gene network orchestrated by PGC-1α. Nevertheless, *ESRRA* expression was similar between fasted individuals with either NGT or type 2 diabetes (Fig. 6i).

Discussion

A link between increased plasma BCAAs and insulin resistance was established as early as 1969 [3], but this association has remained relatively unexplored until the last decade. Here we elucidate the mechanisms underpinning BCAA metabolism in type 2 diabetes. While we

corroborate the association between BCAA metabolites and type 2 diabetes [9, 25-27] and the role of PGC-1α in BCAA catabolism [15, 23, 28], we provide new evidence that an OGTT unmasks impairments in BCAA catabolism in individuals with type 2 diabetes. Moreover, we reveal that PGC-1α-mediated regulation of genes important for BCAA catabolism is dependent on ERRα, a canonical PGC-1α-interacting protein.

Circulating plasma BCAA levels are altered in individuals with type 2 diabetes, however metabolomic profiles of peripheral tissues involved in glucose homeostasis are scarce and the transcriptomic regulation of genes involved in BCAA catabolism is unknown. Studies focusing on skeletal muscle BCAA content are limited to an analysis of adults with insulin resistance [14], rather than type 2 diabetes. We performed untargeted metabolomic analysis on both plasma and *vastus lateralis* biopsies obtained before and after an OGTT from men with either NGT or type 2 diabetes. Corroborating an earlier study of plasma samples from the Framingham Heart Study Offspring cohort [29], circulating BCAAs were decreased after an OGTT and this reduction was attenuated in type 2 diabetes. Concomitantly, we found that this blunted response also affected leucine- and isoleucine-derived BCKAs. In skeletal muscle, insulin inhibits proteolysis [30] and increases the preference for BCAA oxidation [13], which may explain the blunted excursion of BCAA and BCKA metabolites in insulin-resistant individuals with type 2 diabetes as compared to NGT. Consistent with this hypothesis, BCAAs, BCKAs and 3-HIB levels after the glucose challenge were significantly less decreased in the skeletal muscle from individuals with type 2 diabetes. Although we did not detect changes in BCKDHA phosphorylation state, BCAA catabolic flux cannot be predicted by BCKDH phosphorylation status [13], thus, we cannot exclude the possibility that BCKDH activity *per se* is impaired. Moreover, insulin modulates BCAA transamination in type 2 diabetes [31] and BCAT2 activity [32], suggesting that insulin resistance could lead to an accumulation of BCKAs due to defects in both BCAA transamination and oxidation.

Generally, plasma metabolites mirrored skeletal muscle BCAA profile. However, the intramuscular accumulation of isovalerylcarnitine, isobutyrylcarnitine, and 3-HIB was not reflected in plasma, suggesting defects in processes controlling the export of metabolites from myocytes in type 2 diabetes. Accordingly, the accumulation of 3-HIB after an OGTT is notable, since this valine-derived metabolite promotes insulin resistance through increased fatty acid uptake in skeletal muscle [23]. This could lead to a vicious cycle in which secretion of 3-HIB from skeletal muscle may decrease insulin sensitivity and further impair insulin signaling. Although elevated levels of circulating C3 and C5 acylcarnitines have been also detected in individuals with obesity [7], whether accumulation of short-chain acylcarnitines mediates in insulin resistance remains to be elucidated [33]. These results suggest the degradation of BCAA-derived metabolites is incomplete. Additionally, we found a strong correlation of post-OGTT BCAAs and derived BCKAs circulating levels with blood glucose and HbA_{1c}. Since plasma fasting BCAA levels exhibited much weaker relationship with clinical biomarkers of type 2 diabetes, this finding underscores a tight connection between impaired glucose homeostasis and whole-body BCAA catabolism.

The accumulation of BCAA metabolites in individuals with type 2 diabetes was accompanied by reduced expression of genes involved in BCAA catabolism, suggesting that alterations in the transcriptional regulation of these genes could attenuate BCAA catabolism in skeletal muscle. Contrasting a previous report [34], we did not find a correlation between BCAA genes and related metabolites, suggesting that posttranscriptional modifications play a key role in the impairment of BCAA catabolism. Conversely, the BCAA gene set was inversely correlated with blood glucose levels, suggesting a connection between glucose homeostasis and alterations in the transcriptional regulation of genes involved in BCAA catabolism.

PGC-1α mediates the expression of genes involved in BCAA catabolism [15, 23, 28]. Concordantly, expression of *PPARGC1A* was positively correlated with BCAA genes. PGC-

1α also coordinates metabolic and transcriptomic programs linked to cellular energy homeostasis [35-37], and reduced PGC-1α mRNA and protein levels are linked to insulin resistance in type 2 diabetes [38, 39]. In the present study, primary HSMCs and mouse skeletal muscle with reduced *PPARGC1A* expression exhibited a mild reduction in expression of several BCAA genes, whereas PGC-1α overexpression was associated with a consistent upregulation. Thus, while PGC-1α was not essential for basal BCAA gene transcription, a role in the adaptive response to increased BCAA catabolic demands, such as during exercise or nutritional changes cannot be excluded [40]. We next hypothesized that alterations in the BCAA gene network would impact BCAA metabolism. We found that mice overexpressing PGC-1α in skeletal muscle exhibited an upregulation of BCAA genes and reduced intramuscular accumulation of valine, suggestive of increased BCAA catabolic flux. Similarly, adenovirus-mediated overexpression of PGC-1α in C2C12 myotubes increased leucine oxidation rates. However, intramuscular levels of BCAA metabolites were unaltered in PGC-1α mKO mice. Thus, other organs such as adipose tissue may compensate for a putative impairment in BCAA catabolism [41]. Furthermore, a metabolic challenge may be necessary to reveal functional alterations in BCAA metabolism in PGC-1α mKO and mTG mice.

PGC-1α is a transcriptional coactivator and does not directly bind DNA in a sequence-specific manner. The nuclear orphan receptor ERRα is one of the main transcriptional partners of PGC-1α [24], and through this physically interaction, elicits the transcription of genes involved in mitochondrial biogenesis and oxidative phosphorylation [42], lipid metabolism [43] and ketone body homeostasis [44]. We found that *ESRRA* silencing, as well as inhibition of ERRα with an inverse agonist, downregulated BCAA genes and abrogated the PGC-1α-induced responses, indicating ERRα is necessary for the PGC-1α-mediated transcription of BCAA genes. Moreover, *ESRRA* silencing was associated with a modest decrease in BCKDH-stimulated leucine oxidation, suggesting a functional impact of the transcriptional

downregulation of BCAA genes under energy demanding conditions. Thus, we next hypothesized that alterations in ERRα may explain the defects in BCAA catabolism in the individuals with type 2 diabetes. However, expression of *ESRRA* was unaltered in skeletal muscle of individuals with NGT or type 2 diabetes, suggesting that reductions in PGC-1α is sufficient to impair BCAA expression or alternatively, the PGC-1α/ERRα interaction is compromised in type 2 diabetes.

Some limitations of our study warrant discussion. Our analysis was limited to male participants, and therefore we cannot exclude sex-specific differences in the analyzed outcomes. Most of the individuals with type 2 diabetes included in this study were treated with metformin. Considering mitochondria are the major target of metformin, this may affect BCAA metabolism. Due to limitations in the LC/MS methodology, quantitation of BCAA metabolites with CoA moieties was not possible. To overcome this, we used specific derived carnitines from these metabolites as a proxy. Alterations in PGC-1α expression may influence fiber type distribution [19, 45], which could impact the results. Nevertheless, similar results were obtained in transgenic mice, *in vitro* primary HSMCs and C2C12 myotubes, suggesting that alterations in BCAA metabolism are unrelated to fiber type.

In conclusion, altered expression of *PPARGC1A* is associated with disturbances in BCAA metabolism in skeletal muscle of individuals with type 2 diabetes. Experimental approaches to reduce *PPARGC1A* levels partially recapitulates the BCAA gene set profile identified in skeletal muscle from type 2 diabetes patients, without impacting circulating and intramuscular BCAA levels. Our results indicate that glucose loading exacerbates disturbances in the BCAA profile, revealing that the metabolic inflexibility that characterizes type 2 diabetes encompasses BCAA catabolism. Additionally, our data demonstrate that ERRα is essential for PGC-1α-mediated transcriptional regulation of genes involved in BCAA metabolism in primary human myotubes, thereby unraveling a new role for this orphan nuclear receptor.

Data availability. The datasets generated during and/or analyzed during the current study are available from the corresponding author on reasonable request.

Funding. The cost of human metabolomics study was supported by grant from Daiichi Sankyo Co., Ltd. This work was supported by grants from the Novo Nordisk Foundation (NNF14OC0011493, NNF14OC0009941, NNF18CC0034900), Swedish Diabetes Foundation (DIA2018-357), Swedish Research Council (2015-00165, 2018-02389), the Strategic Research Programme in Diabetes at Karolinska Institutet (2009-1068), the Knut and Alice Wallenberg Foundation (2018-0094) and the Stockholm County Council (SLL20170159). David Rizo-Roca is supported by a Novo Nordisk postdoctoral fellowship run in partnership with Karolinska Institutet.

Duality of interest. J.H. is employee of Daiichi Sankyo Co., Ltd.

Author Contributions. R.J.O.S. conceived the idea, planned the experiments and collected and analyzed data. D.R.R performed leucine oxidation assays, analyzed data and wrote the manuscript. A.V.C. contributed to discussion and interpretation of metabolomic and protein data. E.C. collected mouse metabolite data and contributed to discussion. R.F. assisted with animal care, OGTT and skeletal muscle sampling. S.K. contributed to the conception of the idea. J.H. contributed to the conception of the idea. H.K.K. assisted with recruitment and collection of human metabolite data. C.H. provided mouse biological samples and contributed to the discussion of animal data. T.M. supervised acquisition and analysis of mouse metabolite data. A.K. supervised the study and contributed to the discussion of all results. E.N. assisted with recruitment and obtained human skeletal muscle biopsies and blood samples. J.R.Z. supervised the study, edited the manuscript and acquired funding. All authors have reviewed the article and gave their final approval. J.R.Z is the guarantor of this work and, as such, had

full access to all the data in the study and takes responsibility for the integrity of the data and the accuracy of the data analysis.

REFERENCES

[1] Leahy JL (2005) Pathogenesis of type 2 diabetes mellitus. Arch Med Res 36: 197-209

[2] Galgani JE, Moro C, Ravussin E (2008) Metabolic flexibility and insulin resistance. Am J Physiol Endocrinol Metab 295: E1009-1017

[3] Felig P, Marliss E, Cahill GF, Jr. (1969) Plasma amino acid levels and insulin secretion in obesity. N Engl J Med 281: 811-816

[4] Nie C, He T, Zhang W, Zhang G, Ma X (2018) Branched chain amino acids: Beyond nutrition metabolism. Int J Mol Sci 19: 954

[5] Patti ME, Brambilla E, Luzi L, Landaker EJ, Kahn CR (1998) Bidirectional modulation of insulin action by amino acids. J Clin Invest 101: 1519-1529

[6] Huffman KM, Shah SH, Stevens RD, et al. (2009) Relationships between circulating metabolic intermediates and insulin action in overweight to obese, inactive men and women. Diabetes Care 32: 1678-1683

[7] Newgard CB, An J, Bain JR, et al. (2009) A branched-chain amino acid-related metabolic signature that differentiates obese and lean humans and contributes to insulin resistance. Cell Metab 9: 311-326

[8] Wurtz P, Soininen P, Kangas AJ, et al. (2013) Branched-chain and aromatic amino acids are predictors of insulin resistance in young adults. Diabetes Care 36: 648-655

[9] Menni C, Fauman E, Erte I, et al. (2013) Biomarkers for type 2 diabetes and impaired fasting glucose using a nontargeted metabolomics approach. Diabetes 62: 4270-4276

[10] Shah SH, Crosslin DR, Haynes CS, et al. (2012) Branched-chain amino acid levels are associated with improvement in insulin resistance with weight loss. Diabetologia 55: 321-330

[11] Lotta LA, Scott RA, Sharp SJ, et al. (2016) Genetic predisposition to an impaired metabolism of the branched-chain amino acids and risk of type 2 diabetes: A mendelian randomisation analysis. PLoS Med 13: e1002179

[12] Fukagawa NK, Minaker KL, Rowe JW, et al. (1985) Insulin-mediated reduction of whole body protein breakdown. Dose-response effects on leucine metabolism in postabsorptive men. J Clin Invest 76: 2306-2311

[13] Neinast MD, Jang C, Hui S, et al. (2019) Quantitative analysis of the whole-body metabolic fate of branched-chain amino acids. Cell Metab 29: 417-429 e414

[14] Lerin C, Goldfine AB, Boes T, et al. (2016) Defects in muscle branched-chain amino acid oxidation contribute to impaired lipid metabolism. Mol Metab 5: 926-936

[15] Hatazawa Y, Tadaishi M, Nagaike Y, et al. (2014) Pgc-1alpha-mediated branched-chain amino acid metabolism in the skeletal muscle. PLoS One 9: e91006

[16] van Doorn M, Vogels J, Tas A, et al. (2007) Evaluation of metabolite profiles as biomarkers for the pharmacological effects of thiazolidinediones in type 2 diabetes mellitus patients and healthy volunteers. Br J Clin Pharmacol 63: 562-574

[17] Evans AM, DeHaven CD, Barrett T, Mitchell M, Milgram E (2009) Integrated, nontargeted ultrahigh performance liquid chromatography/electrospray ionization tandem mass spectrometry platform for the identification and relative quantification of the small-molecule complement of biological systems. Anal Chem 81: 6656-6667

[18] Al-Khalili L, Chibalin AV, Kannisto K, et al. (2003) Insulin action in cultured human skeletal muscle cells during differentiation: Assessment of cell surface glut4 and glut1 content. Cell Mol Life Sci 60: 991-998
[19] Lin J, Wu H, Tarr PT, et al. (2002) Transcriptional co-activator pgc-1 alpha drives the formation of slow-twitch muscle fibres. Nature 418: 797-801
[20] Lin J, Wu PH, Tarr PT, et al. (2004) Defects in adaptive energy metabolism with cns-linked hyperactivity in pgc-1alpha null mice. Cell 119: 121-135
[21] Chorell E, Ryberg M, Larsson C, et al. (2016) Plasma metabolomic response to postmenopausal weight loss induced by different diets. Metabolomics 12: 1-14
[22] Shaham O, Wei R, Wang TJ, et al. (2008) Metabolic profiling of the human response to a glucose challenge reveals distinct axes of insulin sensitivity. Mol Syst Biol 4: 214
[23] Jang C, Oh SF, Wada S, et al. (2016) A branched-chain amino acid metabolite drives vascular fatty acid transport and causes insulin resistance. Nat Med 22: 421-426
[24] Vernier M, Giguere V (2021) Aging, senescence and mitochondria: The pgc-1/err axis. J Mol Endocrinol 66: R1-R14
[25] Suhre K, Meisinger C, Doring A, et al. (2010) Metabolic footprint of diabetes: A multiplatform metabolomics study in an epidemiological setting. PLoS One 5: e13953
[26] Xu F, Tavintharan S, Sum CF, Woon K, Lim SC, Ong CN (2013) Metabolic signature shift in type 2 diabetes mellitus revealed by mass spectrometry-based metabolomics. J Clin Endocrinol Metab 98: E1060-1065
[27] Yu D, Moore SC, Matthews CE, et al. (2016) Plasma metabolomic profiles in association with type 2 diabetes risk and prevalence in chinese adults. Metabolomics 12
[28] Hatazawa Y, Minami K, Yoshimura R, et al. (2016) Deletion of the transcriptional coactivator pgc1alpha in skeletal muscles is associated with reduced expression of genes related to oxidative muscle function. Biochem Biophys Res Commun 481: 251-258
[29] Ho JE, Larson MG, Vasan RS, et al. (2013) Metabolite profiles during oral glucose challenge. Diabetes 62: 2689-2698
[30] Meek SE, Persson M, Ford GC, Nair KS (1998) Differential regulation of amino acid exchange and protein dynamics across splanchnic and skeletal muscle beds by insulin in healthy human subjects. Diabetes 47: 1824-1835
[31] Halvatsiotis P, Short KR, Bigelow M, Nair KS (2002) Synthesis rate of muscle proteins, muscle functions, and amino acid kinetics in type 2 diabetes. Diabetes 51: 2395-2404
[32] David J, Dardevet D, Mosoni L, Savary-Auzeloux I, Polakof S (2019) Impaired skeletal muscle branched-chain amino acids catabolism contributes to their increased circulating levels in a non-obese insulin-resistant fructose-fed rat model. Nutrients 11
[33] Schooneman MG, Vaz FM, Houten SM, Soeters MR (2013) Acylcarnitines: Reflecting or inflicting insulin resistance? Diabetes 62: 1-8
[34] Hernández-Alvarez MI, Díaz-Ramos A, Berdasco M, et al. (2017) Early-onset and classical forms of type 2 diabetes show impaired expression of genes involved in muscle branched-chain amino acids metabolism. Sci Rep 7: 13850
[35] Estall JL, Kahn M, Cooper MP, et al. (2009) Sensitivity of lipid metabolism and insulin signaling to genetic alterations in hepatic peroxisome proliferator-activated receptor-gamma coactivator-1alpha expression. Diabetes 58: 1499-1508
[36] Wu Z, Puigserver P, Andersson U, et al. (1999) Mechanisms controlling mitochondrial biogenesis and respiration through the thermogenic coactivator pgc-1. Cell 98: 115-124

[37] Yoon JC, Puigserver P, Chen G, et al. (2001) Control of hepatic gluconeogenesis through the transcriptional coactivator pgc-1. Nature 413: 131-138
[38] Moreno-Santos I, Perez-Belmonte LM, Macias-Gonzalez M, et al. (2016) Type 2 diabetes is associated with decreased pgc1alpha expression in epicardial adipose tissue of patients with coronary artery disease. J Transl Med 14: 243
[39] Patti ME, Butte AJ, Crunkhorn S, et al. (2003) Coordinated reduction of genes of oxidative metabolism in humans with insulin resistance and diabetes: Potential role of pgc1 and nrf1. Proc Natl Acad Sci U S A 100: 8466-8471
[40] Hagg SA, Morse EL, Adibi SA (1982) Effect of exercise on rates of oxidation, turnover, and plasma clearance of leucine in human subjects. Am J Physiol 242: E407-410
[41] Herman MA, She P, Peroni OD, Lynch CJ, Kahn BB (2010) Adipose tissue branched chain amino acid (bcaa) metabolism modulates circulating bcaa levels. J Biol Chem 285: 11348-11356
[42] Schreiber SN, Emter R, Hock MB, et al. (2004) The estrogen-related receptor alpha (erralpha) functions in ppargamma coactivator 1alpha (pgc-1alpha)-induced mitochondrial biogenesis. Proc Natl Acad Sci U S A 101: 6472-6477
[43] Luo J, Sladek R, Carrier J, Bader JA, Richard D, Giguere V (2003) Reduced fat mass in mice lacking orphan nuclear receptor estrogen-related receptor alpha. Mol Cell Biol 23: 7947-7956
[44] Svensson K, Albert V, Cardel B, Salatino S, Handschin C (2016) Skeletal muscle pgc-1alpha modulates systemic ketone body homeostasis and ameliorates diabetic hyperketonemia in mice. FASEB J 30: 1976-1986
[45] Handschin C, Chin S, Li P, et al. (2007) Skeletal muscle fiber-type switching, exercise intolerance, and myopathy in pgc-1alpha muscle-specific knock-out animals. J Biol Chem 282: 30014-30021

Table 1. Clinical characteristics of the subjects included in the metabolomic analysis.

	Normal Glucose Tolerance	Type 2 Diabetes	P-value
Age (years)	59 ± 2.4	62 ± 1.2	0.1611
Weight (kg)	81 ± 2.7	88 ± 1.8	0.0209
Height (m)	1.77 ± 0.02	1.79 ± 0.01	0.4082
BMI (kg/m^2)	25.95 ± 0.59	27.66 ± 0.47	0.0307
Waist (cm)	90 ± 1.6	100 ± 1.6	0.0002
Hip (cm)	97 ± 1.2	101 ± 1.2	0.0241
WHR ratio	0.93 ± 0.01	0.99 ± 0.01	0.0008
Pulse (BPM)	62 ± 2.0	68 ± 1.6	0.0234
FP-glucose (mmol/L)	5.41 ± 0.13	8.59 ± 0.37	<0.0001
120 min-glucose (mmol/L)	6.05 ± 0.25	16.66 ± 0.58	<0.0001
HbA_{1c} (mmol/mol)	36.13 ± 1.13	51.19 ± 1.32	<0.0001
HbA_{1c} (%)	5.5 ± 0.10	6.8 ± 0.12	<0.0001
S-insulin (pmol/L)	52.37 ± 5.30	85.51 ± 9.06	0.0124
120 min S-Insulin (pmol/L)	294.2 ± 43.41	327.5 ± 42.06	0.6155
P-Creatinine (µmol/L)	84.53 ± 2.65	80.72 ± 2.17	0.2794
P-ASAT (µkat/L)	0.42 ± 0.04	0.39 ± 0.03	0.5992
P-ALAT (µkat/L)	0.38 ± 0.06	0.48 ± 0.04	0.1161
P-TG (mmol/L)	1.08 ± 0.14	1.41 ± 0.13	0.1093
P-Chol (mmol/L)	5.27 ± 0.17	4.50 ± 0.14	0.0014
P-HDL (mmol/L)	1.33 ± 0.06	1.24 ± 0.06	0.3562
P-LDL (mmol/L)	3.47 ± 0.13	2.62 ± 0.14	0.0003
S-C-peptide (nmol/L)	0.69 ± 0.04	0.99 ± 0.08	0.0115
HOMA1-IR	1.71 ± 0.22	5.28 ± 0.65	0.0013

Results are mean ± SEM for individuals with Normal Glucose Tolerance (n=15) and Type 2 Diabetes (n=26) men. Statistical analysis was performed using Student's *t*-test.

Table 2. Clinical characteristics of the subjects included in the transcriptomic analysis.

	Normal Glucose Tolerance	Type 2 Diabetes	P-value
Age (years)	58 ± 1.8	62 ± 1.3	0.0185
Weight (kg)	84 ± 1.7	89 ± 1.9	0.0314
Height (m)	1.80 ± 0.02	1.79 ± 0.01	0.7185
BMI (kg/m^2)	25.98 ± 0.35	27.94 ± 0.48	0.0020
Waist (cm)	93 ± 1.4	101 ± 1.7	0.0020
Hip (cm)	99 ± 0.9	101 ± 1.3	0.1691
WHR ratio	0.94 ± 0.01	0.99 ± 0.01	0.0009
Pulse (BPM)	61 ± 1.4	68 ± 1.6	0.0072
FP-glucose (mmol/L)	5.46 ± 0.08	8.56 ± 0.39	<0.0001
120 min-glucose (mmol/L)	5.89 ± 0.27	16.20 ± 0.69	<0.0001
HbA_{1c} (mmol/mol)	35.76 ± 0.64	50.44 ± 1.50	<0.0001
HbA_{1c} (%)	5.4 ± 0.06	6.8 ± 0.14	<0.0001
S-insulin (pmol/L)	52.71 ± 5.58	92.58 ± 9.01	0.0008
120 min S-Insulin (pmol/L)	314.9 ± 50.8	350.5 ± 42.4	0.5937
P-Creatinine (µmol/L)	83.64 ± 2.36	79.71 ± 2.29	0.2307
P-ASAT (µkat/L)	0.38 ± 0.03	0.40 ± 0.03	0.7613
P-ALAT (µkat/L)	0.42 ± 0.05	0.50 ± 0.04	0.2565
P-TG (mmol/L)	1.25 ± 0.15	1.43 ± 0.13	0.4415
P-Chol (mmol/L)	5.40 ± 0.20	4.48 ± 0.15	0.0005
P-HDL (mmol/L)	1.30 ± 0.05	1.19 ± 0.06	0.1709
P-LDL (mmol/L)	3.56 ± 0.17	2.63 ± 0.15	0.0002
S-C-peptide (nmol/L)	0.69 ± 0.04	1.03 ± 0.08	0.0008
HOMA1-IR	1.86 ± 0.21	5.23 ± 0.64	<0.0001

Results are shown as mean ± SEM for individuals with Normal Glucose Tolerance (n=25) and Type 2 Diabetes (n=25) men. Statistical analysis was performed using Student's *t*-test.

FIGURE LEGENDS

Figure 1. Flow chart illustrates subject enrolment and analysis. Sixty-one individuals were assessed for eligibility, six of which were excluded for not meeting the inclusion criteria. Group size for transcriptomic and metabolomic analysis is reported. Transcriptomic and metabolomic analysis shared samples from 13 individuals with normal glucose tolerance and 23 with type 2 diabetes subjects.

Figure 2. Glucose loading further attenuates BCAA catabolism in individuals with type 2 diabetes. Boxplots show scaled intensity values of BCAAs **(a-c)**, BCKAs **(d-f)**, BCAA-derived carnitines **(g-k)** and 3-hydroxisobutyrate **(l)** in plasma and skeletal muscle from individuals with NGT (n=15) or type 2 diabetes (n=26), before and after a 120-min OGTT. **m)** Catabolic pathway of BCAA and genes codifying for involved enzymes (in blue boxes). Dashed arrows indicate intermediate metabolites are not shown. **n-p)** Western blot of BCKDHA and pBCKDHA (n = 10 per group). Expression values are expressed as relative to a control sample. Black dots represent outlier values. **q)** Representatives immunoblot of the analyzed proteins in fasting conditions (F) and after an OGTT (O). **r-s)** Spearman correlation coefficients between plasma BCAA metabolites and clinical parameters. Color and size are proportional to correlation strength. **t-w)** Examples of spearman correlation coefficients summarized in panels r and s. Statistical analysis (A-P) was performed using two-way mixed-design ANOVA followed by Sidak's *post-hoc* test. **P*<0.05, ***P*<0.01, ****P*<0.001; †*P*<0.05, ††*P*<0.01, †††*P*<0.001 vs NGT. ‡, condition effect; §, glucose loading effect; ¶, interaction effect. BCAA, branched-chain amino acid; BCKA, branched-chain α-keto acid; KIC, α-ketoisocaproate; KIV, keto-isovaline; KMV, keto-methylvalerate NGT, normal glucose tolerance; SKM, skeletal muscle; T2D, type 2 diabetes. See also ESM Fig. 1.

Figure 3. Expression of genes involved in BCAA catabolism in individuals with type 2 diabetes and correlations with blood glucose levels. a-b) BCAA gene expression in skeletal muscle biopsies of individuals with NGT (n=25) or type 2 diabetes (n=25) before and after a 120-min OGTT. **c)** Expression of the transcriptional coactivator *PGC-1α*. Gene expression is shown as log2(fold-change) relative to the NGT fasting group. Statistical analysis was performed using two-way mixed-design ANOVA followed by Sidak's *post-hoc* test. **d-e)** Spearman correlation coefficients between BCAA genes and clinical parameters (d) or skeletal muscle BCAA metabolites (e) in fasted skeletal muscle. Color and size are proportional to correlation strength; **P*<0.05, ***P*<0.01, ****P*<0.001; †*P*<0.05 vs fasting. ‡, condition effect; §, glucose loading effect. NGT, normal glucose tolerance; T2D, type 2 diabetes; F, fasting. See also ESM Fig. 2.

Figure 4. PGC-1α mediates BCAA gene expression in human skeletal muscle cells. **a)** Efficiency of *PPARGC1A* siRNA-mediated silencing. **b)** Effects of the silencing of *PPARGC1A* on the expression of BCAA catabolic genes, BCKDK and PPM1K. **c)** Expression of *PPARGC1A* in Ad-PGC1A cells. **d)** Effects of Ad-PGC1A on the expression of BCAA catabolic genes, BCKDK and PPM1K. Gene expression is shown as log2(fold-change) relative to the corresponding scramble-treated cells (dotted line). **e-i)** Protein levels of BCKDK **(e)**, PPM1K **(f),** BCKDHA **(g)**, phosphorylated BCKDHA **(h)** and ratio between pBCKDHA and BCKDHA **(i)**. **j)** Representatives immunoblot. Arrow indicates the band corresponding to PPM1K protein. Statistical analysis was performed using paired *t*-test (n=6). **P*<0.05, ***P*<0.01, ****P*<0.001 vs scr (a-b) or Ad-GFP (c-i). siRNA, small interfering RNA; scr, scrambled siRNA; Ad-GFP, adenoviral overexpression of GFP; Ad-PGC1A, adenoviral overexpression of *PPARGC1A*. Red dots, significant outliers not considered in statistical calculations.

Figure 5. Mice with skeletal muscle-specific modified expression of *PPARGC1A* exhibit altered levels of BCAA gene transcripts and related metabolites. a) Quadriceps *PPARGC1A* expression in mKO-PGC1A mice (n=9). **b-d)** Expression of genes encoding BCAT2 and BCKDHA subunits **(b)**, BCKDK and PPM1K **(c)** and BCAA catabolic enzymes **(d)** in mKO mice. **e)** Quadriceps *PPARGC1A* expression in mTG-PGC1A mice (n=6). **f-h)** Expression of genes encoding BCAT2 and BCKDHA subunits **(f)**, BCKDK and PPM1K **(g)** and BCAA catabolic enzymes **(h)** in mTG mice. **i-k)** Scaled intensity values of leucine, isoleucine and valine in plasma from mKO, mTG and correspondent WT littermates. **l-q)** Scaled intensity values of BCAA and downstream intermediate metabolites in mKO, mTG and correspondent WT littermates. Gene expression is shown as log2(fold-change) relative to WT mice. The dotted line represents the mean of the WT group. Statistical analysis was performed using unpaired *t*-test. **P*<0.05, ***P*<0.01, ****P*<0.001 vs WT. WT, wild type; mKO-PGC-1a, muscle-specific PGC-1α knockout mice; mTG-PGC-1a, muscle-specific PGC-1α transgenic mice. See also ESM Fig. S3. SKM, Skeletal Muscle.

Figure 6. PGC-1α regulates BCAA gene transcription through ERRα. a) STRING Interacting Network showing top 5 interacting proteins for PGC-1α. **b)** Efficiency of ERRα silencing in primary HSMCs. **c)** Expression of BCAA genes. **d)** Leucine oxidation rates in HSMCs. Schematic biochemical representation of the leucine oxidation assay is shown. **e)** Expression of *ESRRA*, *PPARGC1A* and target genes in Ad-PGC1A cells transfected with *ESRRA* siRNA. **f-h)** BCAA gene expression in Ad-PGC-1A cells with or without *ESRRA* siRNA. **i)** Expression of *ESRRA* in skeletal muscle biopsies from individuals with NGT or type 2 diabetes. Gene expression is shown as log2(fold-change) relative to the corresponding scramble+GFP treated cells (dotted line) scr (b-c), scr+Ad-GFP (E-H) or NGT Fasting (i). Statistical analysis was performed using paired *t*-test (a-b, n=7), two-way repeated measures ANOVA followed by Tukey's *post-hoc* test (d, n=4; e-h, n=6), or two-way mixed-design

ANOVA followed by Sidak's post-hoc test (i, n=25). *P<0.05, **P<0.01, ***P<0.001 vs scr (a-b) or scr-Ad-GFP (c-f). ‡, siESRRA effect; §, Ad-PGC1A effect; ¶, interaction effect. siRNA, small interfering RNA; Ad-GFP, adenoviral overexpression of GFP; Ad-PGC1A, adenoviral overexpression of *PPARGC1A*; BT2, 3,6-dichlorobrenzo(b)thiophene-2carboxylic acid; scr, scrambled siRNA; TCA, tricarboxylic acid cycle. See also ESM Fig. 4.

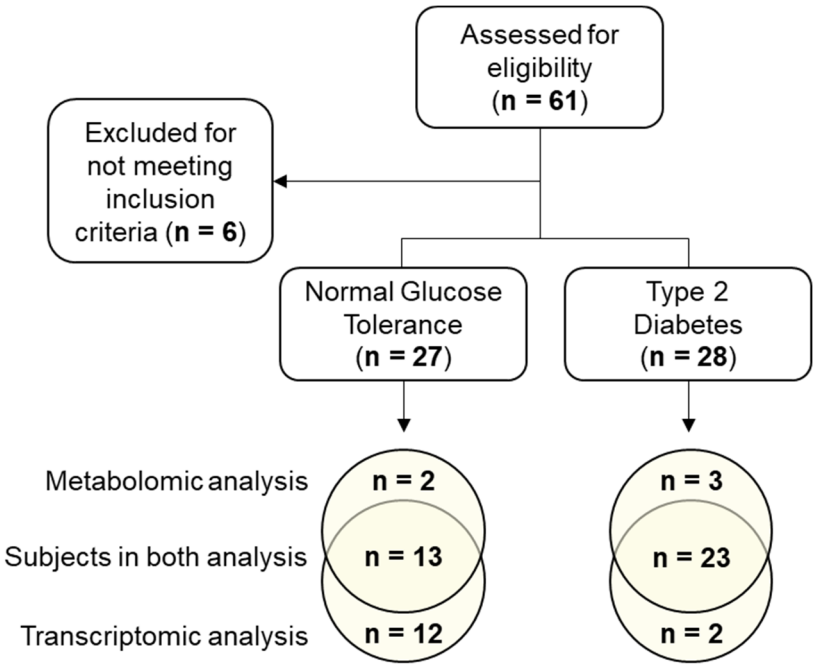
Assessed for eligibility (n = 61)
Excluded for not meeting inclusion criteria (n = 6)
Normal Glucose Tolerance (n = 27)
Type 2 Diabetes (n = 28)
Metabolomic analysis
Subjects in both analysis
Transcriptomic analysis
n = 2
n = 13
n = 12
n = 3
n = 23
n = 2

Figure 1.

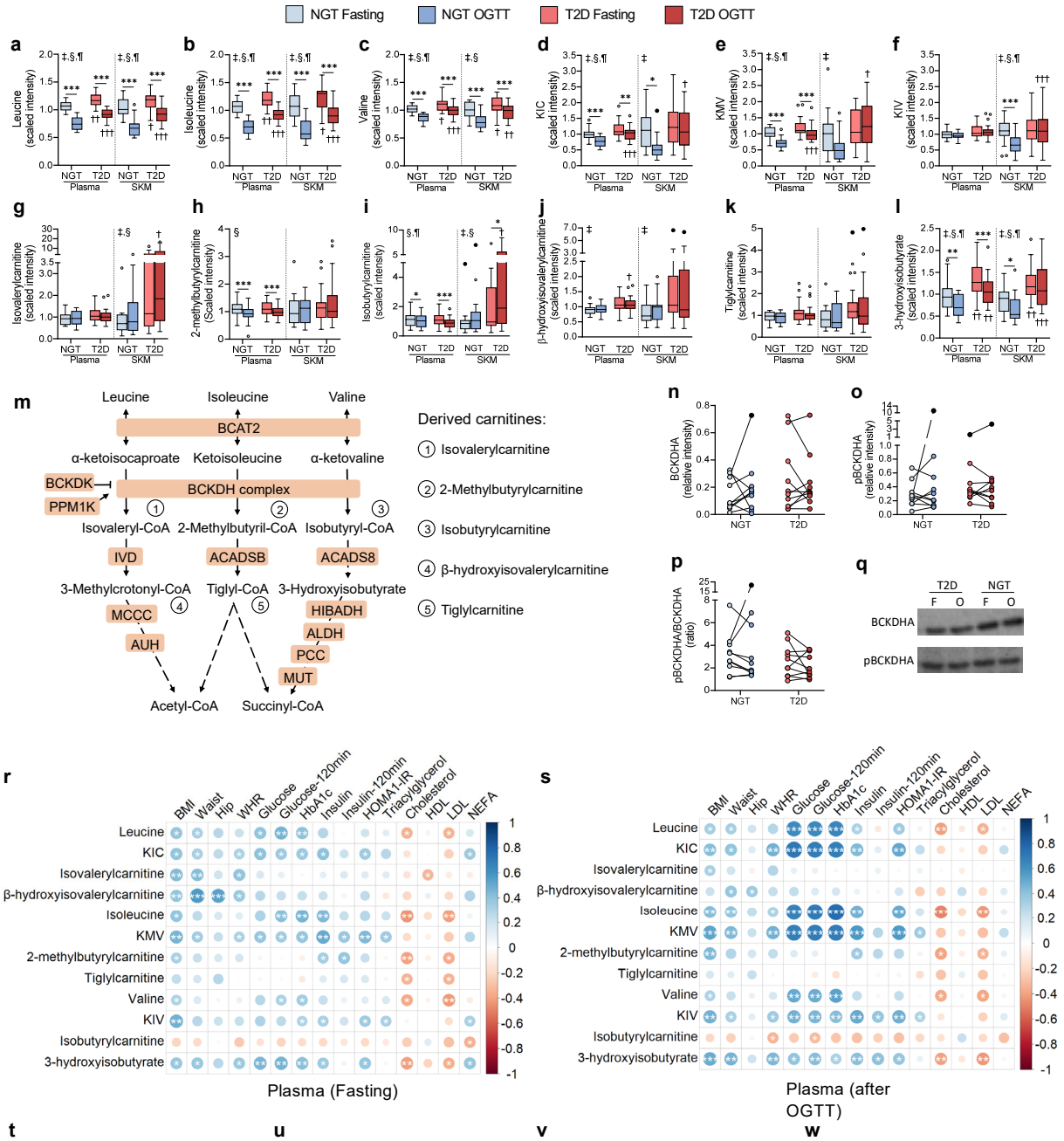
NGT Fasting
NGT OGTT
T2D Fasting
T2D OGTT
Leucine (scaled intensity)
Isoleucine (scaled intensity)
Valine (scaled intensity)
KIC (scaled intensity)
KMV (scaled intensity)
KIV (scaled intensity)
Isovalerylcarnitine (scaled intensity)
2-methylbutyrylcarnitine (Scaled intensity)
Isobutyrylcarnitine (scaled intensity)
β-hydroxyisovalerylcarnitine (scaled intensity)
Tiglylcarnitine (scaled intensity)
3-hydroxyisobutyrate (scaled intensity)
NGT
T2D
Plasma
SKM
Leucine
Isoleucine
Valine
BCAT2
α-ketoisocaproate
Ketoisoleucine
α-ketovaline
BCKDK
PPM1K
BCKDH complex
Isovaleryl-CoA
2-Methylbutyril-CoA
Isobutyryl-CoA
IVD
ACADSB
ACADS8
3-Methylcrotonyl-CoA
Tiglyl-CoA
3-Hydroxyisobutyrate
MCCC
HIBADH
ALDH
AUH
PCC
MUT
Acetyl-CoA
Succinyl-CoA
Derived carnitines:
① Isovalerylcarnitine
② 2-Methylbutyrylcarnitine
③ Isobutyrylcarnitine
④ β-hydroxyisovalerylcarnitine
⑤ Tiglylcarnitine
BCKDHA (relative intensity)
pBCKDHA (relative intensity)
pBCKDHA/BCKDHA (ratio)
T2D
NGT
F
O
BCKDHA
pBCKDHA
BMI
Waist
Hip
WHR
Glucose
Glucose-120min
HbA1c
Insulin
Insulin-120min
HOMA1-IR
Triacylglycerol
Cholesterol
HDL
LDL
NEFA
Plasma (Fasting)
Plasma (after OGTT)
KIC (scaled intensity)
KMV (scaled intensity)
Glucose (120 min)
HOMA-IR
r=0.71
r=0.68
r=0.52
r=0.56

Figure 2.

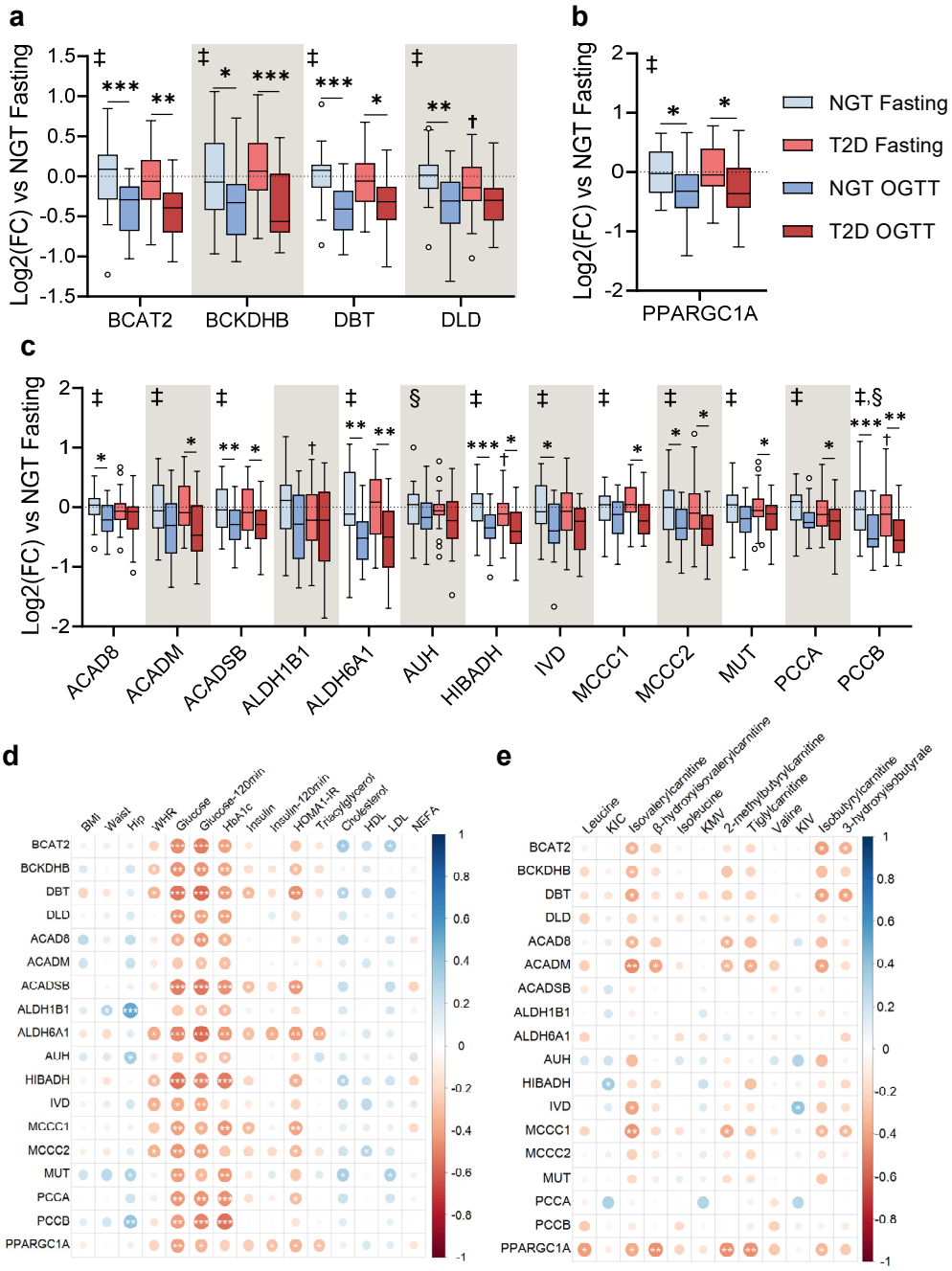
a
Log2(FC) vs NGT Fasting
BCAT2
BCKDHB
DBT
DLD
b
PPARGC1A
NGT Fasting
T2D Fasting
NGT OGTT
T2D OGTT
c
ACAD8
ACADM
ACADSB
ALDH1B1
ALDH6A1
AUH
HIBADH
IVD
MCCC1
MCCC2
MUT
PCCA
PCCB
d
BMI
Waist
Hip
WHR
Glucose
Glucose-120min
HbA1c
Insulin
Insulin-120min
HOMA1-IR
Triacylglycerol
Cholesterol
HDL
LDL
NEFA
e
Leucine
KIC
Isovalerylcarnitine
β-hydroxyisovalerylcarnitine
Isoleucine
KMV
2-methylbutyrylcarnitine
Tiglylcarnitine
Valine
KIV
Isobutyrylcarnitine
3-hydroxyisobutyrate

Figure 3.

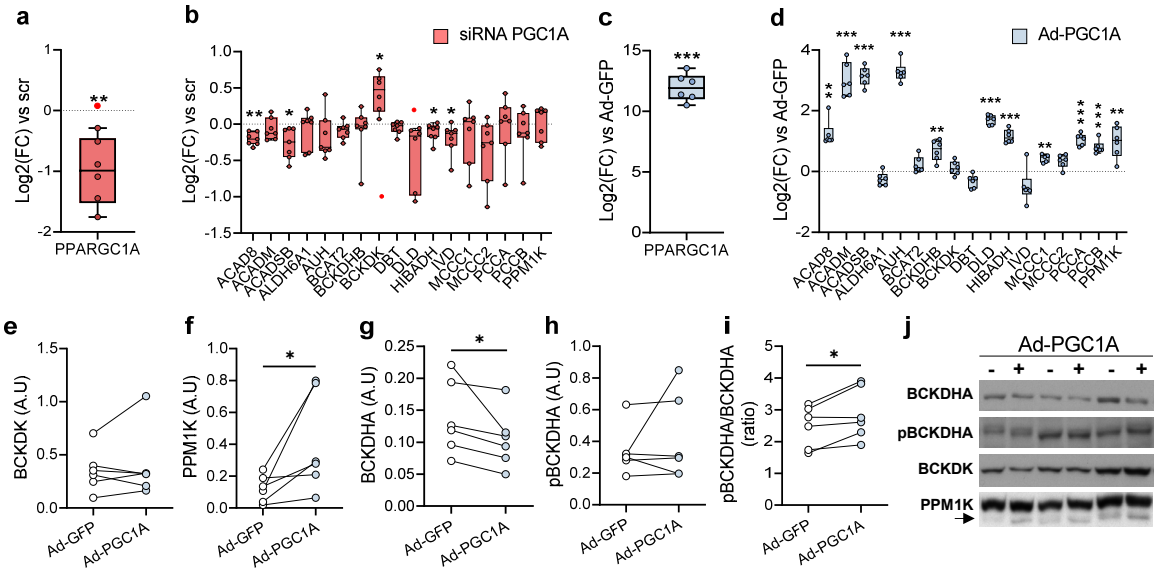
a
Log2(FC) vs scr
PPARGC1A
b
siRNA PGC1A
Log2(FC) vs scr
ACAD8
ACADM
ACADSB
ALDH6A1
AUH
BCAT2
BCKDHB
BCKDK
DBT
DLD
HIBADH
IVD
MCCC1
MCCC2
PCCA
PCCB
PPM1K
c
Log2(FC) vs Ad-GFP
PPARGC1A
d
Ad-PGC1A
Log2(FC) vs Ad-GFP
e
BCKDK (A.U)
f
PPM1K (A.U)
g
BCKDHA (A.U)
h
pBCKDHA (A.U)
i
pBCKDHA/BCKDHA (ratio)
Ad-GFP
Ad-PGC1A
j
Ad-PGC1A
BCKDHA
pBCKDHA
BCKDK
PPM1K

Figure 4.

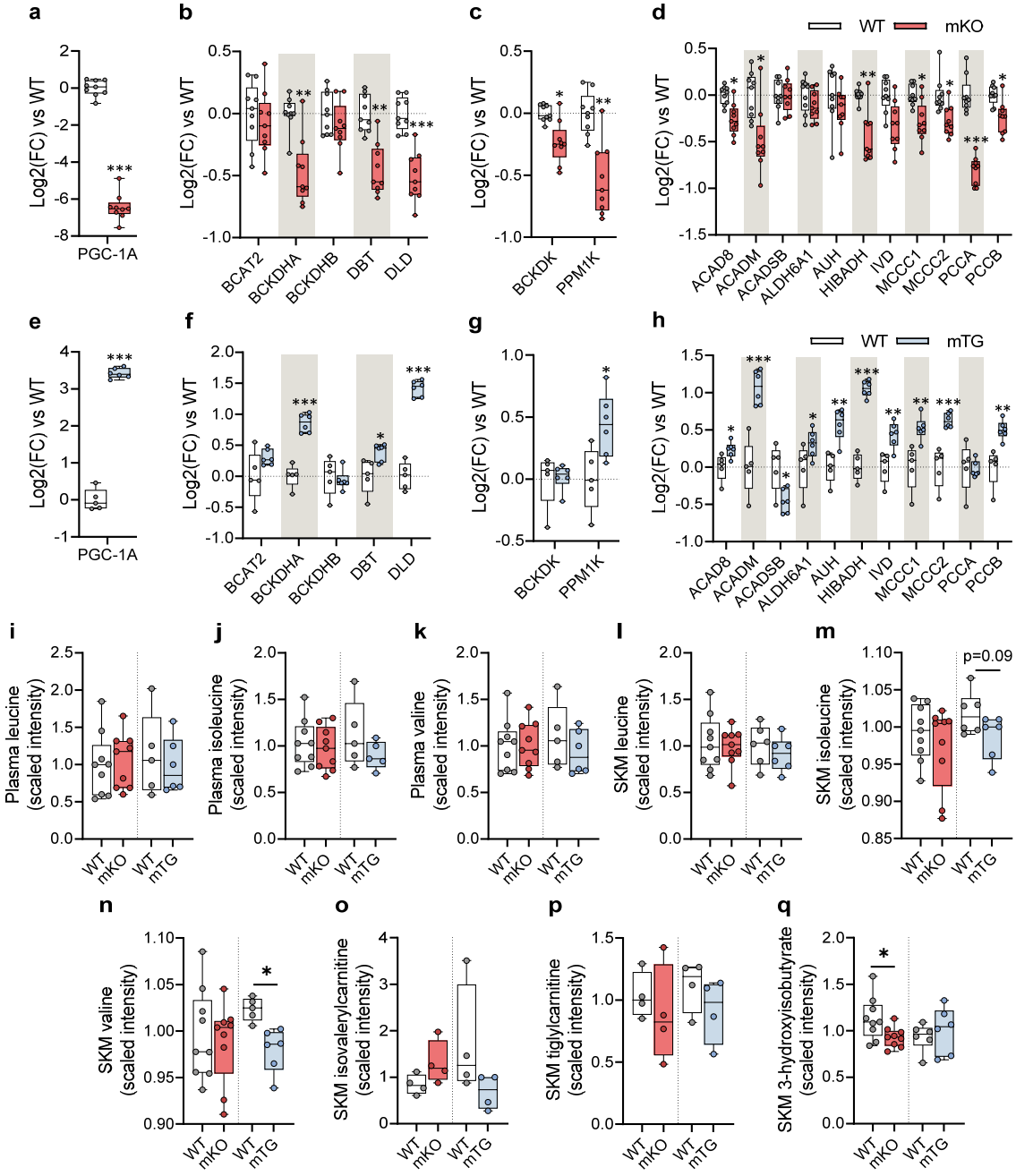
a
b
c
d
e
f
g
h
i
j
k
l
m
n
o
p
q
Log2(FC) vs WT
PGC-1A
BCAT2
BCKDHA
BCKDHB
DBT
DLD
BCKDK
PPM1K
ACAD8
ACADM
ACADSB
ALDH6A1
AUH
HIBADH
IVD
MCCC1
MCCC2
PCCA
PCCB
WT
mKO
mTG
Plasma leucine (scaled intensity)
Plasma isoleucine (scaled intensity)
Plasma valine (scaled intensity)
SKM leucine (scaled intensity)
SKM isoleucine (scaled intensity)
p=0.09
SKM valine (scaled intensity)
SKM isovalerylcarnitine (scaled intensity)
SKM tiglylcarnitine (scaled intensity)
SKM 3-hydroxyisobutyrate (scaled intensity)

Figure 5.

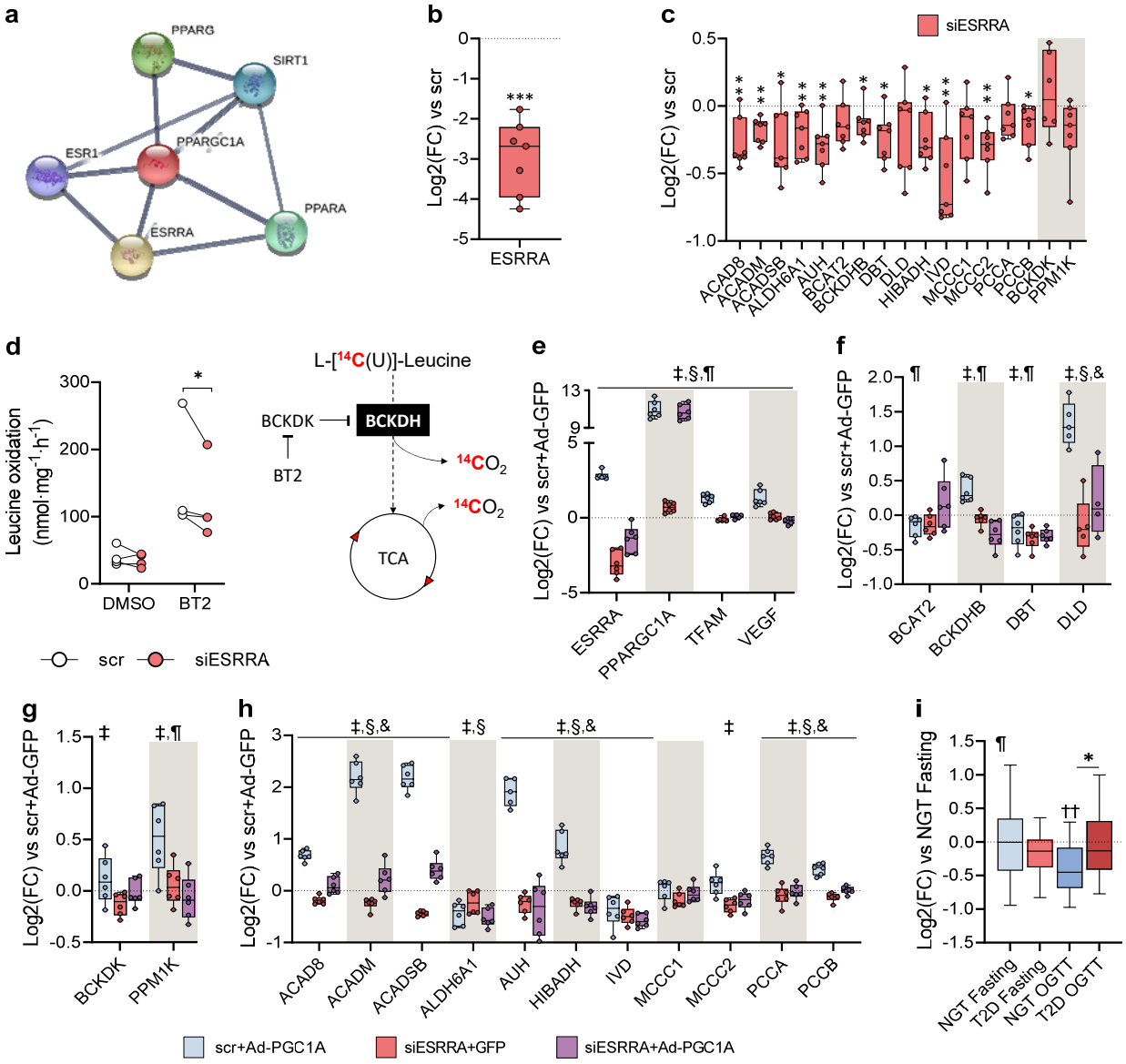
a
PPARG
SIRT1
ESR1
PPARGC1A
PPARA
ESRRA
b
Log2(FC) vs scr
ESRRA
c
siESRRA
Log2(FC) vs scr
ACAD8
ACADM
ACADSB
ALDH6A1
AUH
BCAT2
BCKDHB
DBT
DLD
HIBADH
IVD
MCCC1
MCCC2
PCCA
PCCB
BCKDK
PPM1K
d
Leucine oxidation (nmol·mg-1·h-1)
DMSO
BT2
L-[14C(U)]-Leucine
BCKDK
BCKDH
BT2
14CO2
TCA
scr
siESRRA
e
Log2(FC) vs scr+Ad-GFP
ESRRA
PPARGC1A
TFAM
VEGF
f
Log2(FC) vs scr+Ad-GFP
BCAT2
BCKDHB
DBT
DLD
g
Log2(FC) vs scr+Ad-GFP
BCKDK
PPM1K
h
Log2(FC) vs scr+Ad-GFP
ACAD8
ACADM
ACADSB
ALDH6A1
AUH
HIBADH
IVD
MCCC1
MCCC2
PCCA
PCCB
i
Log2(FC) vs NGT Fasting
NGT Fasting
T2D Fasting
NGT OGTT
T2D OGTT
scr+Ad-PGC1A
siESRRA+GFP
siESRRA+Ad-PGC1A

Figure 6.

Sjögren et al. Branched-Chain Amino Acid Metabolism is Regulated by ERRα in Primary Human Myotubes and is Further Impaired by Glucose Loading in Type 2 Diabetes.

Electronic Supplementary Materials (ESM)

ESM Methods

Human plasma and skeletal muscle metabolomics

Metabolomic analysis was performed by Metabolon, Inc. (Durham, NC, USA) as described (20). Equal volume of plasma and equal weights of *vastus lateralis* biopsy were used for all samples. The protein fraction was removed using a methanol extraction method while allowing maximum recovery of small molecules. The resulting extract was divided into five fractions: one for analysis by ultra-high-performance liquid chromatography-tandem mass spectroscopy (UPLC-MS/MS) with positive ion mode electrospray ionization, one for UPLC-MS/MS with negative ion mode electrospray ionization, one for liquid chromatography (LC) polar platform, one for gas chromatography–MS (GC–MS), and one sample was reserved as a backup.

The LC/MS portion of the UPLC-MS/MS platform was based on a Waters ACQUITY UPLC and a Thermo Scientific Q-Exactive high resolution/accurate mass spectrometer interfaced with a heated electrospray ionization source and Orbitrap mass analyzer operated at 35,000 mass resolution. Separated dedicated columns (Waters UPLC BEH C18-2.1x100 mm, 1.7 µm) were used to perform analysis under acidic positive ion optimized conditions and basic negative ion optimized conditions. The third aliquot was analyzed via negative ionization following elution from a HILIC column (Waters UPLC BEH Amide 2.1x150 mm, 1.7 µm) using a gradient consisting of water and acetonitrile with 10 mM ammonium formate.

Samples destined for GC-MS analysis were dried under vacuum for at least 18 h prior to being derivatized under dried nitrogen using bistrimethyl-silyltrifluoroacetamide. Derivatized samples were separated on a 5% diphenyl / 95% dimethyl polysiloxane fused silica column (20

m x 0.18 mm ID; 0.18 µm film thickness) with helium as carrier gas and a temperature ramp from 60°C to 340°C within a 17.5-min period. Samples were analyzed on a Thermo-Finnigan Trace DSQ fast-scanning single-quadrupole mass spectrometer using electron impact ionization and operated at unit mass resolving power. The scan range was from 50–750 m/z.

Compounds were identified by comparison to library entries of purified standards or recurrent unknown entities. Metabolon maintains a library based on authenticated standards that contains the retention time/index (RI), mass to charge ratio (m/z), and chromatographic data on all molecules present in the library. Biochemical identifications were based on three criteria: retention index within a narrow RI window of the proposed identification, accurate mass match to the library and the MS/MS forward and reverse scores between the experimental data and authentic standards. The MS/MS scores were based on a comparison of the ions present in the experimental spectrum to the ions present in the library spectrum.

Mouse plasma and skeletal muscle metabolomics

Mouse sample preparation and analysis was performed at the Swedish Metabolomics Centre (Umeå University). Prior to gas chromatography time-of-flight mass spectrometry (GC-TOF/MS) analysis, a two-step derivatization procedure was carried out to increase metabolites volatility and reduce number of tautomeric forms. Derivatized samples were analyzed on an Agilent 6890 gas chromatograph equipped with a 10 m × 0.18 mm i.d. fused silica capillary column with a chemically bonded 0.18-µm DB 5-MS stationary phase (J&W Scientific, Folsom, CA, USA). The injector temperature was 270°C. The column temperature was held at 70°C for 2 min, increased by 40°C min^{-1} to 320°C, and held there for 1 min. The column effluent was introduced into the ion source of a Pegasus III time-of-flight mass spectrometer, GC-TOF/MS (Leco, St. Joseph, MI, USA). The transfer line and ion source temperatures were

250°C and 200°C, respectively. Ions were generated by a 70-eV electron beam at an ionization current of 2.0mA. Spectra were recorded in the mass range 50–800 m/z at 30 spectra s^{-1}.

Samples destined to liquid chromatography time-of-flight mass spectrometry (LC-TOF/MS) were re-suspended in methanol and water (1:1) and injected onto a Waters Acquity UPLC HSS T3 C18 column (2.1 × 50 mm, 1.8 µm; Waters Corporation, Milford, MA, USA) in combination with a 2.1 mm x 5 mm, 1.8 µm VanGuard precolumn (Waters Corporation) held at 40°C. Metabolites chromatographic separation were carried out using a gradient solvent system consisting of water with 0.1% formic acid and acetonitrile/isopropanol (75/25, v/v) with 0.1% formic acid at a flow rate of 0.5 mL min^{-1}. The detection of separated metabolites was performed using the Agilent 6550 Q-TOF mass spectrometer equipped with a jet stream electrospray ionization source, operating in both positive and negative ion modes. A reference interface was connected for accurate mass measurements; the reference ions purine (4 µM) and HP-0921 (Hexakis (1H, 1H, 3H-tetrafluoropropoxy) phosphazine) (1 µM) were infused directly into the MS at a flow rate of 0.05 mL min-1 for internal calibration. Full scan MS spectra were collected in a centroid mode over the mass range 70-1700 m/z with an acquisition rate of 4 spectra s^{-1}. The Auto MS/MS was performed on QC-samples. The isolation width was set to narrow, i.e. approx. 1.3 amu, the mass range was 40-1700, and data was collected in centroid mode with an acquisition rate of 3 scans s-1. The collision energy was 10, 20 and 40 ev. Data were acquired with MassHunter Acquisition Software B.07.01.

The processing of GC-TOF/MS data and extraction of putative metabolites was conducted as described (21). Briefly, an in-house MATLAB script was used for the extraction of putative metabolites by matching the mass spectra and retention indices to in-house mass spectral library at the Swedish Metabolomics Centre and the publicly available Max Planck Institute library in Golm. The processing of LC-TOF/MS data and extraction of putative metabolites and lipids were performed by MassHunter Profinder version B.08.00 in combination with

Qualitative Analysis software version B.07.00, PCDL manager version B.07.00 and Mass Profiler Professional™ 13.0 (all from Agilent Technologies Inc., Santa Clara, CA, USA). Annotation of metabolites were done by matching the retention time (MS and MS-MS spectra) against the in-house metabolite library.

RNA isolation and relative mRNA expression

Total RNA from human skeletal muscle biopsies, mouse skeletal muscles and cultured myotubes was extracted using TRIzol according to manufacturer's instructions (Thermo Fisher Scientific). Concentration and extraction quality (A260/A280) of RNA samples were determined by spectrophotometry using a Nanodrop ND-1000 (Thermo Fisher Scientific) and equal amounts of RNA were used for cDNA synthesis. cDNA was synthesized using the High Capacity cDNA Reverse Transcription kit with random primers (4368814, Thermo Fisher Scientific). RT-qPCR was performed using either a ViiA 7 Real-Time PCR 384-well system or a StepOne Plus Real-Time PCR 96-well system (Thermo Fisher Scientific). Gene expression was determined using Fast SYBR™ Green Master Mix (4309155, Thermo Fisher Scientific). Sequences of primers used for the real-time PCR are reported in ESM Tables 1 and 2. Gene expression in human skeletal muscle biopsies and cultured myotubes was normalized to the geometrical mean of *GUSB*, *RPLP0* and *TBP* expression. For C2C12 cells and mouse tibialis anterior muscle, gene expression was normalized to the geometrical mean of *B2M*, *RPLP0* and *TBP* expression. Relative gene expression was calculated by the comparative ΔΔCt method and normalized to control group (in human and mouse samples, NGT Fasting and WT mice, respectively) or control samples (*in vitro* experiments, cells from each donor were normalized against their correspondent siRNA scr-treated counterparts).

Western blot analysis

Human skeletal muscle biopsies were homogenized in ice-cold lysis buffer [137 mM NaCl, 2.7 mM KCl, 1 mM MgCl2, 0.5 mM Na_3VO_4, 10% (vol/vol) glycerol, 1% (vol/vol) Triton X-100, 20 mM Tris, 10 mM NaF, 1 mM EDTA, 1 mM PMSF, and 1% (vol/vol) protease inhibitor cocktail set 1 (Merck, Darmstadt, Germany)] using a TissueLyser II (21 Hz, 45 sec, two times. Qiagen, Haan, Germany). Homogenates were rotated for 30 min at 4°C and thereafter subjected to centrifugation at 12000 g for 15 min at 4°C. Cells were lysed in ice-cold homogenization buffer. Lysates were rotated for 30 min at 4°C and subjected to centrifugation at 12000 g for 15 min at 4°C.

Protein concentration in the supernatants of skeletal muscle homogenates and cell lysates was determined by BCA protein assay kit (Pierce Biotechnology, Rockford, IL, USA). Samples were prepared with Laemmli buffer to equal final protein concentrations, separated on Criterion XT Bis-Tris Gels for SDS-PAGE (Bio-Rad, Hercules, CA; USA) and transferred to PVDF membranes (Merck). Thereafter, membranes were stained with Ponceau S to verify transfer quality and confirm equal protein loading. After blocking with 7.5% nonfat milk in Tris-buffered saline with Tween (TBST; 10 mM Tris·HCl, 100 mM NaCl, 0.02% Tween 20) for 2 h at room temperature, membranes were incubated overnight at 4°C with primary antibodies against β-actin (A5441, Sigma-Aldrich), GAPDH (sc-47724, Santa Cruz Biotechnology), BCKDHA (ab68094, Abcam), p^{S293}-BCKDHA (ab200577, Abcam), BCKDK (sc-374425, Santa Cruz Biotechnology), and PPM1K (ab67935, Abcam), all at a 1:1000 dilution. Antibodies were validated in HSMCs in which the corresponding encoding gene was silenced with siRNA. Membranes were washed with TBST and incubated with horseradish peroxidase-conjugated secondary antibodies (1:10000 – 1:25000). Proteins were visualized by enhanced chemiluminescence (Amersham ECL Western Blotting Detection Reagent, Little Chalfont, UK). Bands of interest were semi-quantified by densitometry (QuantityOne, Bio-Rad).

ESM Tables

ESM Table 1. Forward and reverse sequences of primers used in gene expression experiment analysis of human skeletal muscle.

Gene	Forward sequence (5' to 3')	Reverse sequence (5' to 3')
ACAD8	CAGGAGGAGAGGAAGGATGC	AGTGTGGGTTCTACTCCTGA
ACADM	ACCAGACCTGTAGTAGCTGC	GAATCAACCTCCCAAGCTGC
ACADSB	AGGCTGCTAAGAAGAAATTTCCT	GTAAATGTTTGCAGGGGAGC
ALDH1B1	AACCAGAACCCAAGCGTGAT	GCTGGTTGTAGGGGATGTCT
ALDH6A1	GAACTGCCATCTTCACCACC	TGGATGCCCTGTTTGCCATA
AUH	TGATATACGAGTAGCAGCTTCCT	CCCTCCTGGTTCTGTTCCA
B2M	TGTCTTTCAGCAAGGACTGG	AGCAAGCAAGCAGAATTTGG
BCAT2	CGCTCCTGTTCGTCATTCTC	CTAACACGGTGGGCCCATA
BCKDHB	GAGAGGTAGCTTCCATGGCA	TGATTTCCGATGCAAAGCCG
BCKDK	TAACGCCCACCATGATGCT	GCCTGGTCCTTGATCGGA
DBT	AAAACAACTGCTGCTCTCCG	TGCTATCAAACTGAGACACTGT
DLD	TGGTGCAGGAGTAATAGGTGT	GCTTTACCACCAGAAGCAGC
ESRRA	ACTATGGTGTGGCATCCTGT	CCGGACAGCTGTACTCGAT
HIBADH	AGCAGTTTTCATGGATGCCC	AACAGCTCCACAGTACACCA
IVD	CACTTCCAGTTGATGCAGGG	AAACACTGAATGCCGTCCAG
GUSB	CAGAGCGAGTATGGAGCAGA	ACTCTCGTCGGTGACTGTTC
MCCC1	GGGAGACTGCACTTACCTGA	TCCAGCTTTGACAAACACCTT
MCCC2	GGAGGTGGCATTATTACAGGC	TGCTCCTCCCGAATCAACTA
MUT	GCCCTCTTTTCCAGACTCCT	GGTATCACCCCTCCACACAT
PCCA	TGATGAAGAGACCAGGGATGG	TCGAGTCTCCGCATCCAAAA
PCCB	CGATCCCAGTGACCGTCTG	TCCAACAGTCCTCCCATTCA
PPARGC1A	TCTGAGTCTGTATGGAGTGACAT	CCAAGTCGTTCACATCTAGTTCA
PPM1K	AAGCCTTTTCGAGTCATGCC	GCTGCCCCAAACTATTCCAA
TBP	AACAACAGCCTGCCACCTTA	GCCATAAGGCATCATTGGAC
TFAM	CTGTCTTGGCAAGTTGTCCA	CAACGCTGGGCAATTCTTCT
VEGFA	CAGAAGGAGGAGGGCAGAAT	CATCAGGGGCACACAGGAT

ESM Table 2. Forward and reverse sequences of primers used in gene expression analysis of mouse skeletal muscle.

Gene	Forward sequence (5' to 3')	Reverse sequence (5' to 3')
ACAD8	GGCTACGGCTATCTGAAGGA	CCTGAAGCAGGTTTCGAGAG
ACADM	GCCCAGAGAGCTCTAGACGA	GTTCAACCTTCATCGCCATT
ACADSB	AAGCCTTGCGAGCTTAACAG	TCCAAGGAGACAAGCAGGTT
ALDH6A1	CTTCTGGATGGGCGAAGAAT	TGTTTCTGTCTCCAAAACCACA
AUH	GCAATTAACCAAGGGATGGA	AGCGAGGAGGTCTTTTCTCC
B2M	TTCTGGTGCTTGTCTCACTGA	CAGTATGTTCGGCTTCCCATTC
BCAT2	TACGTCATTCTGTGCCCTGT	CCTCTCTTCTGGGCTTCTCG
BCKDHA	GGCCGGATCTCCTTCTACAT	TAGTCCCGGTACATGAGCAC
BCKDHB	GGTAATACCCCGAAGCCCTT	AGGGTTCTACTGGGACCTGT
BCKDK	GCTACATGAAGACAAGCCTGA	GCATGGGAATGAAGGGGAAC
DBT	CGCGTGGAATCAAACTCTCC	CCCAATGTTGTGAGAAGCCTT
DLD	GGCATGGTGAAGATTCTTGG	GAAGCACCATATTCCAATGC
HIBADH	GGGAGCTGTTTTCATGGACG	CATTCCAGCAACTCTTGGGC
IVD	TCGATATTGCCTGTGGACGA	GGGGCCAGGTTCTCTTGAA
MCCC1	TCCAGTGAGTGCAGAAGGAG	ACCATCAGAGAGTCTCCAGC
MCCC2	CAACTTACCTCGGCAAGCAG	GTACAGGAGCCCATGACCAC
PCCA	GCATCCAGTTTCTTGGCACA	TCTGCTACCATGTCTCCAGG
PCCB	TCCTGAGCTGGACACAGTTG	TTTTTGCGTAACTGGGCATT
PPARGC1A	TATGGAGTGACATAGAGTGTGCT	CCACTTCAATCCACCCAGAAAG
PPM1K	ACAAGGATTAAGCTCTACCATGC	GTGCTGTTGTCTTCGGTACC
RPLP0	AGATTCGGGATATGCTGTTGGC	TCGGGTCCTAGACCAGTGTTC
TBP	CCTTGTACCCTTCACCAATGAC	ACAGCCAAGATTCACGGTAGA

ESM Table 3. Y-intercept p-values corresponding to the analysis of covariance comparing individuals with normal glucose tolerance and type 2 diabetes controlling for variation in BMI and age.

	BMI		Age	
	Plasma	**SKM**	**Plasma**	**SKM**
Leucine	<0.0001	0.0008	<0.0001	<0.0001
Isoleucine	<0.0001	0.0008	<0.0001	<0.0001
Valine	0.0013	0.0092	0.0003	0.0006
α -ketoisocaproate	0.0014	0.0300	0.0002	0.0024
Ketoisoleucine	0.0021	0.0175	0.0403	0.0106
α-ketovaline	0.1540	0.0184	0.0431	0.0011
Isovalerylcarnitine	0.4343	0.0166	0.1120	0.0199
2-methylbutyrylcarnitine	0.9525	0.1697	0.1535	0.1250
Isobutyrylcarnitine	0.5386	0.0244	0.4478	0.0189
β-hydroxyisovalerylcarnitine	0.3515	0.0625	0.3134	0.0370
Tiglylcarnitine	0.8905	0.1711	0.5280	0.2819
3-hydroxyisobutyrate	0.0132	0.0116	0.0008	0.0006

Linear regression between BCAA metabolites and BMI/Age was calculated in the two experimental groups (after OGTT). Obtained slopes were in all cases not statistically different between groups, allowing to compare Y-intercepts of the regression lines.

ESM Figures

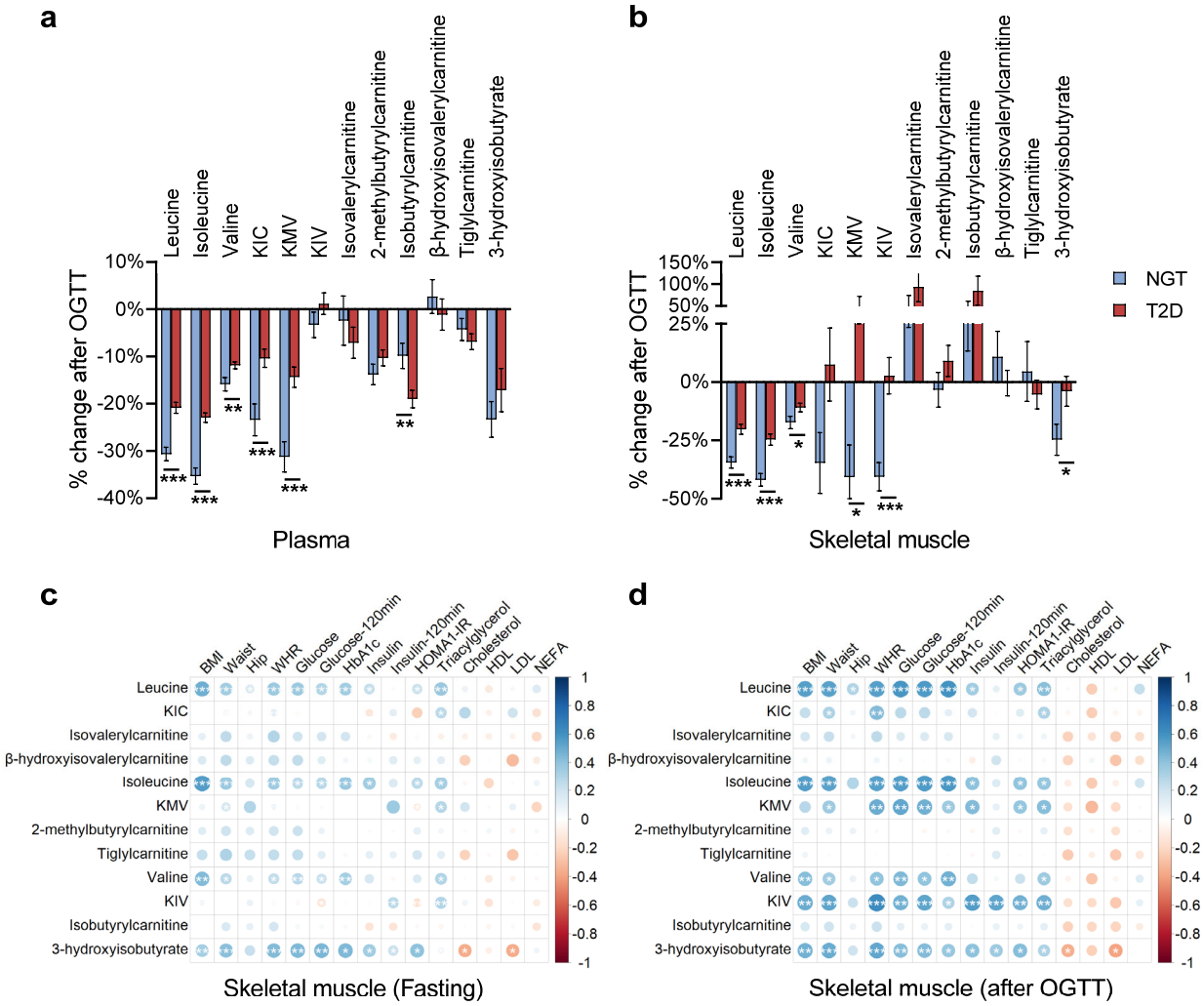

ESM Figure 1 (Supplementary to Figure 2). a-b) Metabolite excursions after OGTT in individuals with normal glucose tolerance (NGT) and type 2 diabetes (T2D). **c-d)** Spearman correlation coefficients between clinical parameters and skeletal muscle BCAA metabolites measured before (**c**) and after (**d**) and OGTT. Color and size are proportional to correlation strength; *, $P<0.05$, **, $P<0.01$ and ***, $P<0.001$. KIC, α-ketoisocaproate; KIV, keto-isovaline; KMV, keto-methylvalerate.

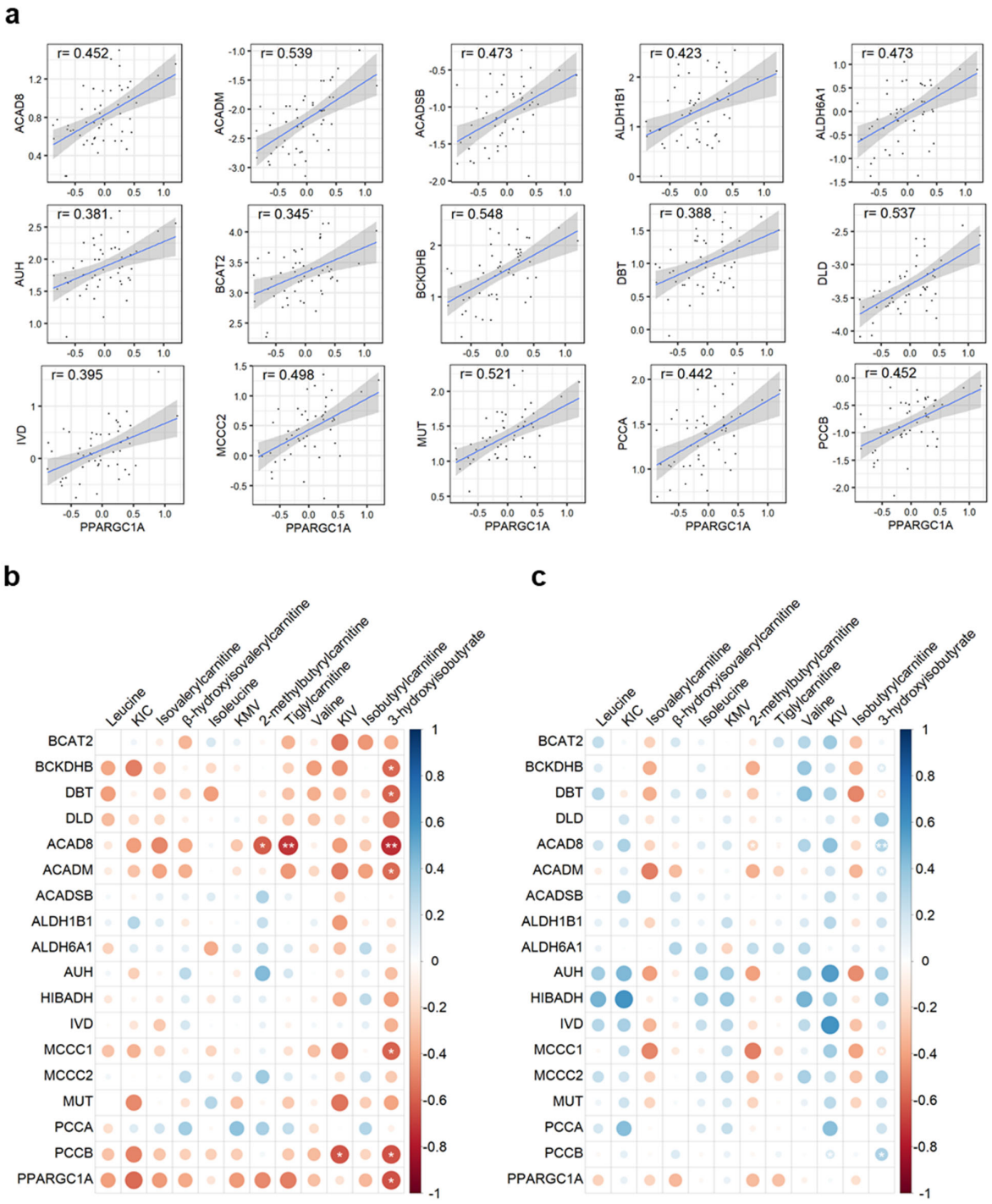

ESM Figure 2 (Supplementary to Figure 2). a) Spearman correlation between the skeletal muscle expression of *PPARGC1A* and BCAA genes. **b-c)** Spearman correlation coefficients between expression of genes involved in BCAA catabolism and skeletal muscle BCAA metabolites measured in individuals with normal glucose tolerance (**b**) and with type 2 diabetes (**C**). Color and size are proportional to correlation strength; *, $P<0.05$, **, $P<0.01$ and ***, $P<0.001$. KIC, α-ketoisocaproate; KIV, keto-isovaline; KMV, keto-methylvalerate.

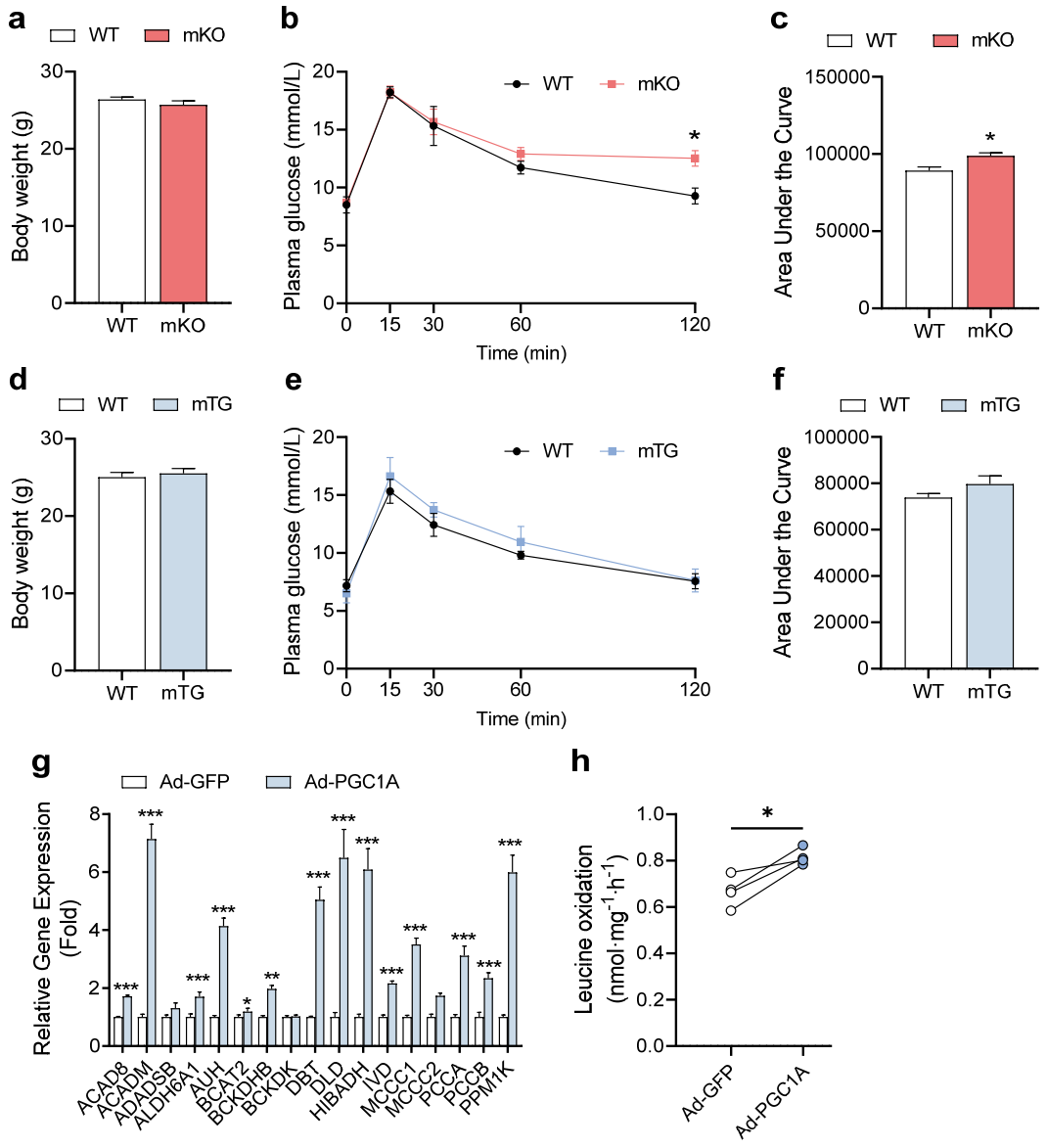

ESM Figure 3 (Supplementary to Figure 5). Mouse glucose tolerance and BCAA gene expression in *PPARGC1A* overexpressing C2C12 myotubes. a) Body weight of mKO mice and WT littermates (n=9). **b-c)** Oral glucose tolerance test and corresponding area under the curve of mKO animals and WT littermates (n=4). **d)** Body weight of mTG mice and WT littermates (n=6). **e-f)** Oral glucose tolerance test and corresponding area under the curve of mTG mice and WT littermates (n=4). **g)** BCAA gene expression in Ad-PGC1A C2C12 myotubes (n=4). **h)** Leucine oxidation in Ad-PGC1A C2C12 myotubes (n=4). *, $P<0.05$; **, $P<0.01$ and ***$P<0.001$. Results are expressed as mean ± SEM. Ad-GFP, adenoviral overexpression of green fluorescent protein; Ad-PGC1A, adenoviral overexpression of PPARGC1A.

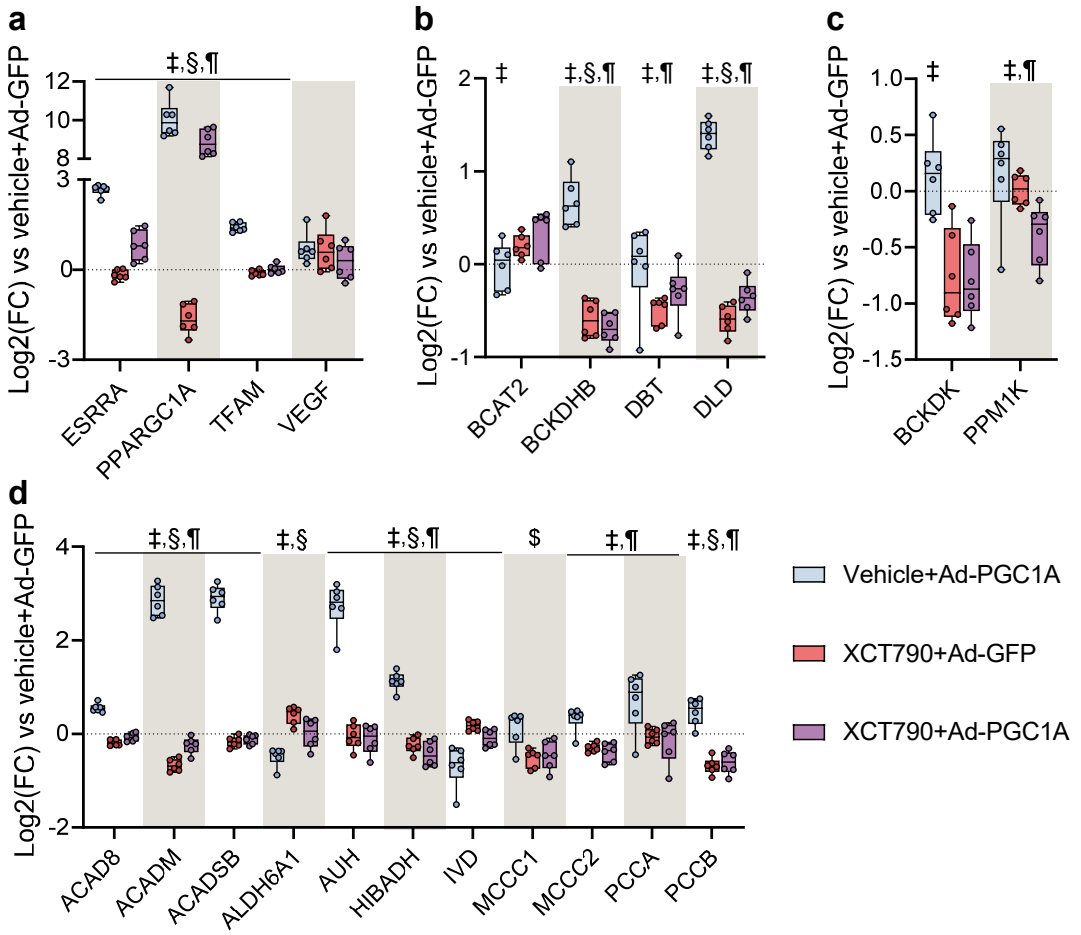

ESM Figure 4 (Supplementary to Figure 6). Effects of ERRα inverse agonist on BCAA gene expression. a) Expression of *ESRRA, PPARGC1A* and target genes in Ad-PGC1A cells treated with the ERRα inverse agonist XCT-790. **b-d)** BCAA gene expression in Ad-PGC1A cells treated with vehicle or XCT-790. Gene expression is shown as log2(fold-change) normalized to the scr+Ad-GFP (dotted line). Statistical analysis was performed using paired t-test (A-C, n=7) or two-way repeated measures ANOVA followed by Tukey's *post-hoc* test (C-F, n=6). ‡, XCT-790 effect; §, Ad-PGC1A effect; ¶, interaction effect. siRNA, small interfering RNA; scr, scrambled siRNA; Ad-GFP, adenoviral overexpression of green fluorescent protein, Ad-PGC1A, adenoviral overexpression of *PPARGC1A*.